Geochemistry at U. S. National Laboratories

Oak Ridge National Laboratory

David R. Cole, David J. Wesolowski, James G. Blencoe, Juske Horita, Lee R. Riciputi, Mostafa Fayek, Lawrence M. Anovitz, and Scott Brooks

INTRODUCTION

Oak Ridge National Laboratory (ORNL) is the U. S. Department of Energy's largest science and energy laboratory (www.ornl.gov). Managed since April 2000 by a partnership of the University of Tennessee and Battelle, ORNL was established in 1943 as a part of the secret Manhattan Project. During the 1950s and 1960s, ORNL was an international center for the study of nuclear energy and related research in the physical and life sciences. The creation of the Department of Energy in the 1970s led to an expansion of ORNL's research program into areas of energy production, transmission, and conservation. The laboratory's six major core competencies include neutron science, energy, high performance computing, complex biological systems, advanced materials, and national security. The laboratory is comprised of a number of research divisions, as well as numerous centers and institutes. Consistent with the national scientific trend of an emphasis in genetics, nanoscience, and advanced computing, ORNL is undergoing an expansion involving the completion of several new facilities including the Functional Genomics Center, the Center for Nanophase Materials Science, the Advanced Materials Characterization Laboratory, and the Joint Institute for Computational Science. Additionally, the $1.4 billion Spallation Neutron Source, slated for completion in 2006, will make ORNL one of the world's foremost centers for neutron science research.

The earliest roots of geochemical research at ORNL reach back into the 1940s and 50s in two distinct arenas; one involved issues of waste disposal, characterization of actinides in environmental systems, and radionuclide transport in both soil and groundwater environments, and the second involved the pioneering studies of the properties of high-temperature water and salt solutions as nuclear reactor coolants and geothermal energy sources. Despite the absence of a centralized Geosciences division, activities in these areas had a profound impact on waste mitigation policy/procedures and hydrothermal geochemistry, respectively. As one of the world's leading centers for experimental studies of the properties of hydrothermal fluids, including water and steam, it was inevitable that a geochemistry research program would grow from this fertile ground because water is the primary transporter of mass and energy in the crust. Similarly, a world-class program designed to quantitatively constrain the deleterious impact of toxic and radioactive contaminants on water quality and biological systems was spawned from the early pioneering efforts to assess the environmental consequences of both low- and high-level radioactive waste disposal.

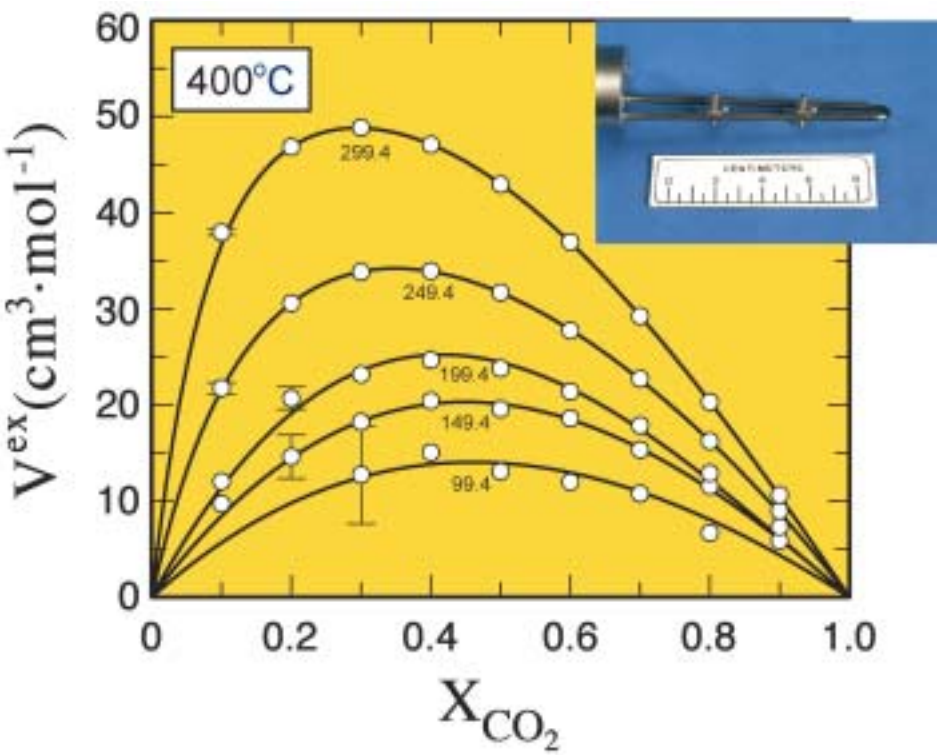

Fig. 1 Experimentally determined excess molar volumes (V^{ex}) of CO_2-H_2O mixtures at 400°C and pressures below (99.4 – 299.4 b) the critical isochore of pure H_2O. The plot symbols depict our experimental data (with error bars), and the curves represent interpolation functions used to illustrate the general trends of the isobaric data. The inset shows a close-up of the vibrating tube.

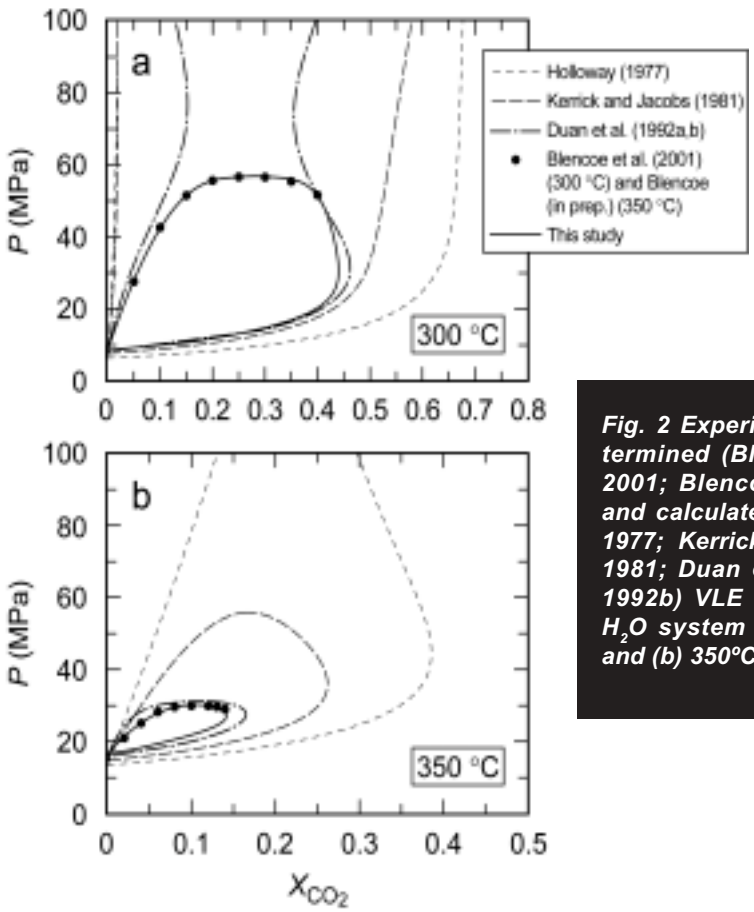

Fig. 2 Experimentally determined (Blencoe et al. 2001; Blencoe, in prep.) and calculated (Holloway 1977; Kerrick and Jacobs 1981; Duan et al. 1992a, 1992b) VLE for the CO_2-H_2O system at (a) 300ºC and (b) 350ºC.

Currently, geochemistry activities at ORNL are divided between the Chemical Sciences Division (CSD) and the Environmental Sciences Division (ESD). In CSD, the research staff focuses primarily on model systems involving complex natural fluids and their interactions and reactions with solids from ambient conditions to elevated temperatures and pressures. In this program, the effort can be subdivided into three thrust areas, each with its own unique problems and methods for addressing these problems.

• fluid-dominated processes involving complex geological fluids;
• the properties and processes uniquely associated with fluid/fluid and fluid/solid interfaces; and
• complex heterogeneous mineral-fluid reactions involving processes such as dissolution/precipitation, mineral replacement, grain boundary and lattice diffusion, and fluid confinement in nanoporous regimes.

Scientists in (ESD) focus on understanding processes and issues of importance to Earth's shallow environment and ecological systems. A subset of the Division's research portfolio can be grouped under the broad heading of Environmental Geochemistry. Research strengths in geosciences, environmental chemistry, hydrology, biogeochemistry, and environmental biotechnology are integrated to conduct research in the environmental sciences. Research efforts conducted at the lab to field scale provide a sound scientific basis for identifying problems, advancing remediation technologies, and evaluating the success of such approaches.

Below we present a number of scientific highlights from these four areas that best define the geochemistry activity at ORNL.

COMPLEX GEOLOGIC FLUIDS

Experimental studies of homogeneous aqueous chemistry at elevated temperatures and pressures has a long history at ORNL, beginning in the early days of the former Reactor Chemistry Division in the 1950's with the pioneering studies by M. Lietzke on the activity coefficients of the acid halides, the hydrolysis of cations by C. Baes, R. E. Mesmer and F. Sweeton, the vapor pressures of concentrated electrolytes by Mesmer and H. Holmes, the conductances of dilute electrolytes by W. Marshall and the high temperature heat of dilution calorimetry studies of Mesmer and R. Busey (see Mesmer et al., 1997 and references therein). This work has been continued in the Aqueous Chemistry and Geochemistry Group by physical chemists J. M. Simonson, D.A. Palmer and M. Gruszkiewicz and expanded to a very fruitful collaboration with geochemists D.J. Wesolowski, J.G. Blencoe, D.R. Cole, J. Horita and former group members S.E. Drummond and P. B n zeth. Thus, the early interest in metal speciation and pH-control in steam generator systems has evolved into applications in geothermal energy, hydrocarbon resources, seafloor hydrothermal systems, ore deposits, CO_2 sequestration and the assessment of toxic and radioactive

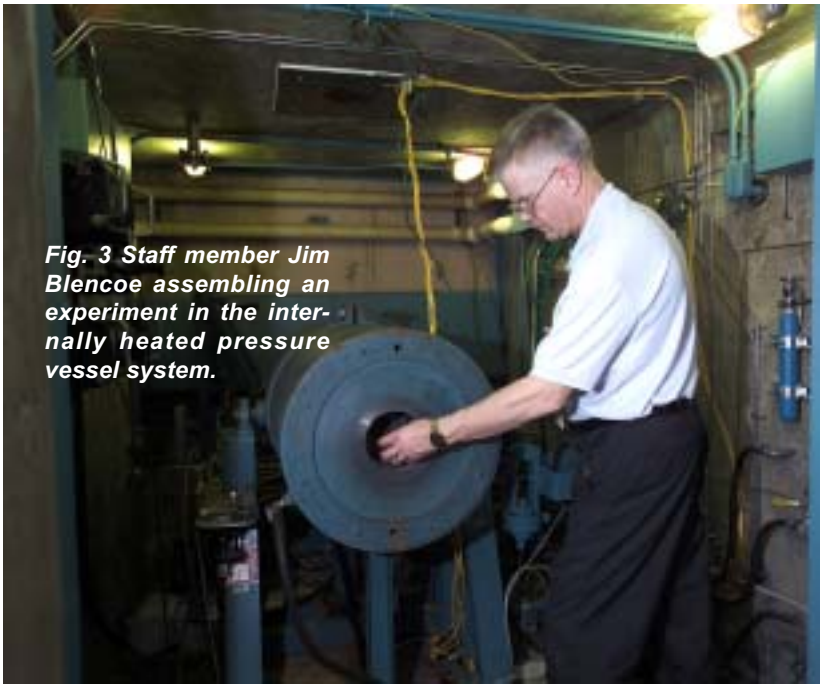

Fig. 3 Staff member Jim Blencoe assembling an experiment in the internally heated pressure vessel system.

waste disposal and remediation schemes. For a recent compilation of ORNL's high temperature aqueous chemistry and geochemistry studies and experimental techniques, the interested reader is directed to chapters in the recent book on *Aqueous Systems at Elevated Temperatures and Pressures: Physical Chemistry in Water, Steam and Hydrothermal Solutions* (Palmer et al., 2004).

The overarching goal of this thrust area is to develop a comprehensive understanding of the thermophysical properties, structures, dynamics, and reactivities of complex geologic fluids and molecules (water and other C-O-H-N-S fluids, electrolytes, and organic-biological molecules) at multiple length scales (molecular to macroscopic) over wide ranges of temperature, pressure, and composition. This knowledge is foundational to advances in the understanding of other geochemical processes involving mineral-fluid interfaces and reactions. Our approach is to interrogate the macroscopic properties and molecular-level forces and interactions of geochemically relevant fluids at representative near-surface and crustal conditions. A quantitative understanding of the causative relationships between macroscopic properties and key molecular-level interactions will impact our ability to predict more complex geochemical behavior in natural fluids over wider ranges of environmental conditions.

Thermophysical Properties:

Jim Blencoe and his collaborators use state-of-the-art laboratory devices to determine the thermodynamics and phase relations of CO_2-CH_4-N_2-H_2O-NaCl fluids at elevated temperatures and pressures. Thermophysical properties and phase behavior are quantified with unsurpassed precision and accuracy. A unique, high temperature, high pressure, vibrating-tube

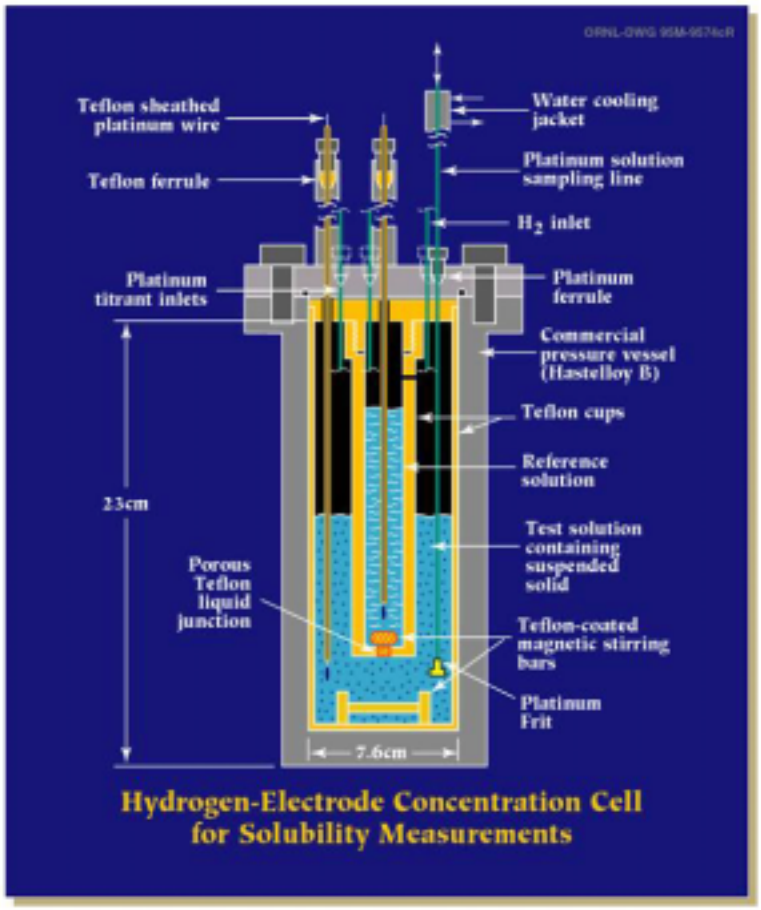

Fig. 4 Schematic of typical ORNL hydrogen electrode concentration cell configuration. A nested set of Teflon cups contain the reference solution (of known pH) and the test solution being studied. Teflon-sheathed platinum wires extend into each solution, serving as the rigorously-Nernstian electrodes. Both solutions are exposed to the same H_2 partial pressure, and there for the difference in potential is described by DE = (RT/F)ln(aH^+_{ref}/aH^+_{test}) - E_{lj} where E_{lj} is the potential drop across the liquid junction formed by a porous Teflon plug in the bottom of the reference cup. Both cups contain Teflon-coated magnetic stirring bars. One or more platinum capillary inlets are included, allowing addition of titrants from zircalloy positive displacement pumps. The cell shown contains a platinum dip tube with an in situ platinum submicron filter for removing samples during homogeneous or heterogeneous experiments.

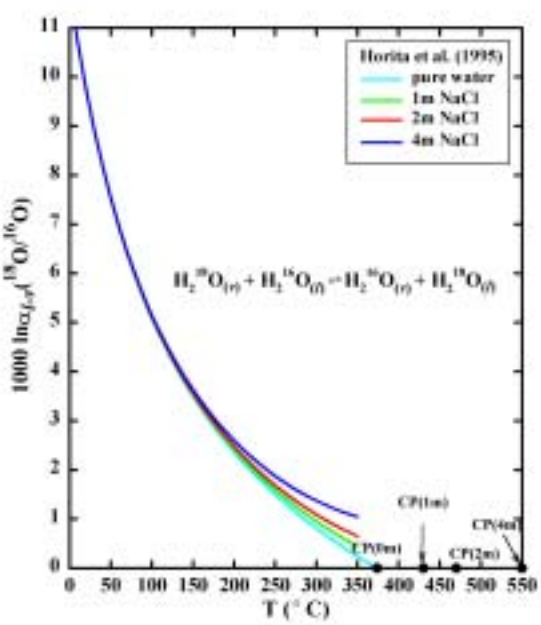

Fig. 5 The effect of dissolved NaCl on $^{18}O/^{16}O$ fractionation between liquid water and water vapor (Horita et al., 1995).

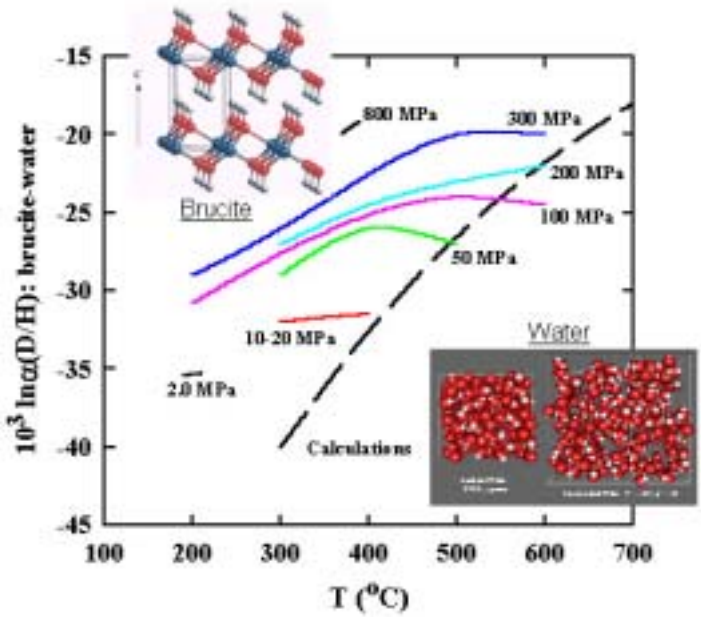

Fig. 6 The effect of pressure on D/H fractionation between brucite, $Mg(OH)_2$, and water (Horita et al., 2002).

densimeter (VTD) is employed to determine the volumetric properties of binary and ternary CO_2-CH_4-N_2-H_2O mixtures at 50-400º C (Fig. 1) (Blencoe et al., 1996). To date, results have been reported for binary and ternary CO_2-CH_4-N_2 gases, and for binary, aqueous CO_2-N_2-H_2O fluids (e.g. Seitz and Blencoe, 1999; Blencoe et al., 1999). An oscillating Inconel U-tube (Fig. 1) is the heart of the VTD. The tube is operable at *P-T* conditions as high as 120 MPa and 500º C. Properly configured and energized, the tube behaves as a harmonic oscillator, with the period of vibration varying monotonically with fluid density. Reported densities for pure fluids are believed to be accurate to ±0.0005 g/cm^{-3}. Estimated uncertainties for fluid mixtures range from ±0.0005 g/cm^3(~1.0%) for low-density fluids to ±0.0010 g/cm^3(~0.15%) for high-density mixtures.

The VTD can also be used to determine the upper baric stabilities of liquid-vapor assemblages (vapor-liquid equilibria, VLE) in fluid systems at high subcritical temperatures (Fig. 2) (Blencoe et al., 2001). The first step is to create an isobaric-isothermal, physically isolated and chemically homogeneous sample of "high-pressure" fluid of known composition. Fluid pressure is then lowered slowly at constant temperature. Pressure readings and matching values for (the period of vibration of the U-tube) are recorded at 1 or 2 bar intervals. When the fluid begins to separate into two phases (liquid + vapor), a distinct inflection is observed in the trend of *P* vs. *T*. Performing such experiments for mixed-volatile fluids at closely spaced compositional intervals produces a complete high-*P* liquid-vapor boundary curve/surface that is accurate to approximately ±2 bars.

The heterogeneous phase equilibria and activity-composition relations of binary and ternary fluid ± "salt" (CO_2-N_2-H_2O-NaCl) systems at 500-1000º C and pressures to 3000 bars are being determined with a custom-designed, hydrogen-service, internally heated pressure vessel (IHPV, Fig. 3) (Anovitz et al., 1998; 2004a). The IHPV is a unique apparatus for conducting experiments at moderate-to-high temperatures and pressures, and at low-to-very-high hydrogen fugacities. In its current configuration, the vessel can be operated routinely at temperatures between 22 and 1000ºC, and at hydrogen fugacities as high as 300 MPa. Many different kinds of samples (encapsulated rocks, minerals, gases, and liquids; pure metals and alloys; and numerous types of ceramics and polymer materials) can be reacted in the working cavity near the center of the vessel; therefore, the IHPV has great practical utility in numerous key areas of geochemical, petrologic, metallurgical, ceramic and hydrogen research, including: the activity-composition relations, multicomponent phase equilibria, and reaction kinetics of rock-forming crystalline solutions, mixed-volatile fluids, and brines at crustal temperatures and pressures; redox-sensitive, high *P-T* fluid/rock interactions; diffusion of hydrogen through solids; and production and consumption of hydrogen by solids and liquids. A key advantage of the ORNL IHPV is that it can be used to fix the activity of water in encapsulated samples. This is done by controlling the fugacities of hydrogen and oxygen (fH_2 and fO_2) inside each capsule, which automatically fixes water activity by the equilibrium: $H_2 + O_2 = H_2O$. Oxygen fugacity is fixed internally in each capsule by the addition of a solid buffer, usually Ni-NiO or Co-CoO. Hydrogen fugacity is mea-

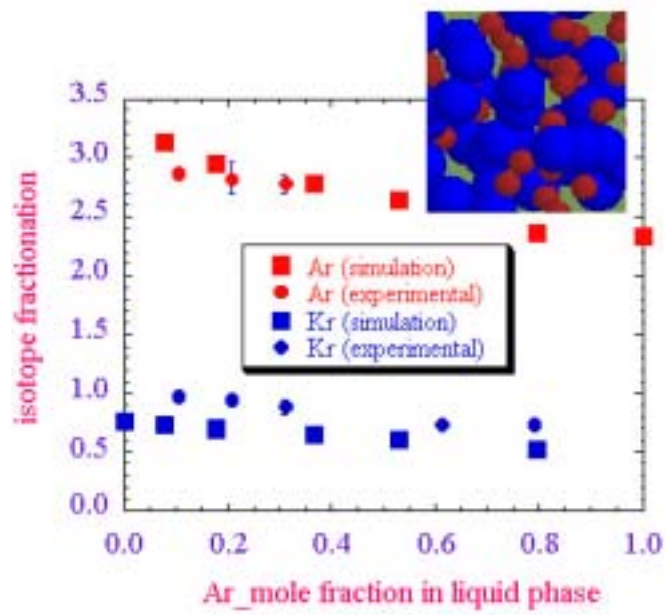

Fig. 7 Molecular-based simulations by means of advanced computing technologies are critical to our fundamental understanding of isotopic fractionation of various geologic-planetary systems. This figure presents the first ever simulations of mixtures (upper inset: Ar-red, Kr-blue) show good agreements of liquid-vapor fractionation of $^{40}Ar/^{36}Ar$ and $^{84}Kr/^{80}Kr$ in the system Ar-Kr with experiments in the literature (lower figure) (Chialvo and Horita, 2003).

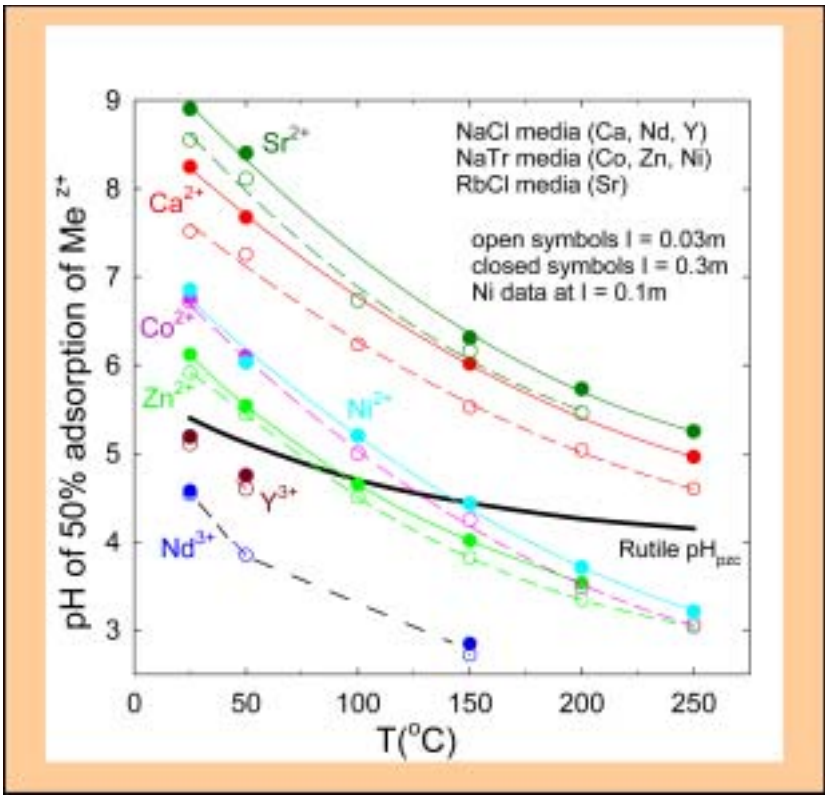

Fig. 8 Plot of the pH at which 50% of a trace multivalent cation is sorbed on the surface of a rutile powder suspension in the pH-cell shown in Figure 4. In all of these experiments, approximately 50 grams of a solution containing 0.001molal Me^{z+} and 0.001 molal H^+ in the background electrolyte type and ionic strength indicated, was initially placed in the test cup along with about 1 gram of the rutile (Tioxide, Corp., 15m²/g surface area, pretreated as described by Machesky et al., 2001). Samples were removed for analysis during titration to higher pH to establish the sorption isotherm and the 50% adsorption value. The pH of zero net surface charge of rutile is also shown as a function of temperature (Machesky et al., 2001).

sured with a Shaw membrane. Use of a pre-mixed gas reduces hydrogen gradients in the vessel, allowing a constant hydrogen fugacity to be rapidly achieved and maintained until the experiment is quenched, and permits a range of water activities to be obtained.

The equations of state (EOS) developed from these experimental studies are used in predicting fluid behavior in a diverse range of environments such as oil, gas and geothermal reservoirs, volcanic systems, pipelines, high temperature treatment of wastes (supercritical oxidation processes), and CO_2 disposal in geological formations such as depleted oil and gas reservoirs and coal-beds (Blencoe et al., 2000; Labotka et al., 2002; Blencoe, 2004). The lower temperature results obtained by Blencoe and his colleagues have direct relevance to the use of CO_2 to displace CH_4 from unmineable coal seams, a value-added technology for CO_2 sequestration under serious consideration by DOE.

In Situ pH Studies:

Dave Wesolowski has made extensive use of ORNL's unique high temperature hydrogen electrode cells (Mesmer et al., 1970), which enable continuous, highly accurate and long-term pH-monitoring (Fig. 4) of both homogeneous and heterogeneous aque-

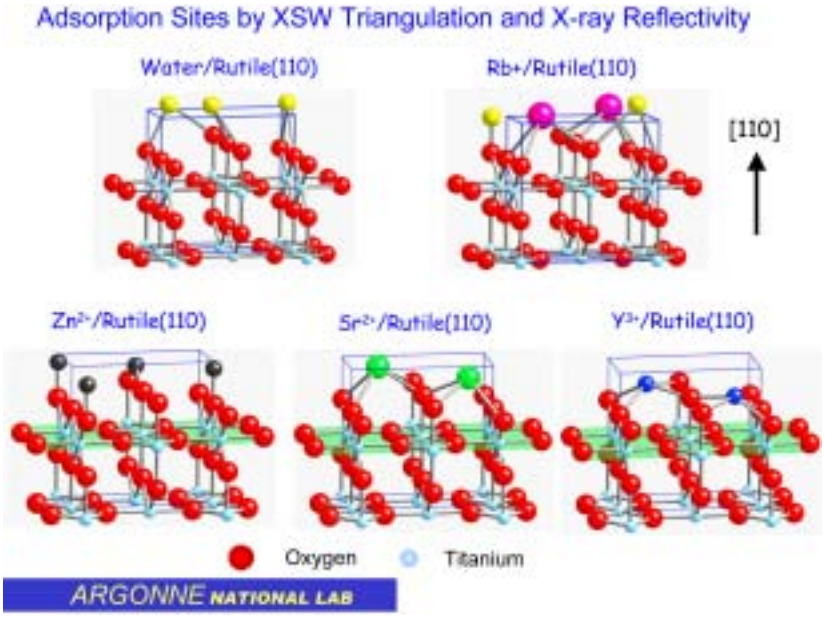

Fig. 9 Inner sphere adsorption sites of ions on the rutile (110) surface determined by synchrotron X-ray standing wave and crystal truncation rod studies. These sites are in good agreement with similar sorption positions obtained in MD simulations, with the exception of Zn^{2+}, for which we are still working to optimize the MD simulations based on new ab initio studies that indicate a coordination change from 6- to 4-fold upon sorption. Not only do the ions occupy specific sorption sites relative to the underlying crystal structure, but the first layer of water molecules also occupy lattice-related sites and are observed by MD simulation to be highly oriented and essentially unable to diffuse away from the surface, at least in the simulation time frame.

ous reactions from 0-300˚C at pressures near vapor saturation and hydrogen partial pressures from fractions of an atmosphere to approximately 100 atmospheres. This technique has enabled the definitive studies of the dissociation constants of nearly all of the major organic and inorganic weak acids and bases, including water itself, that control the pH of industrial and subsurface aqueous solutions, as well as the hydrolysis constants of many of the most important metals in NaCl and KCl brines. Numerous visiting chemists and geochemists have worked with Wesolowski and Palmer to extend our knowledge of even the most basic geochemical reactions. Just a few examples include the dissociation constants of HSO_4^- and citric acid (Dickson et al., 1990; Benezeth et al., 1997), the complexation of Al^{3+} by SO_4^{2-} (Ridley et al., 1999; Xiao et al., 2002) and the hydrolysis of Nd^{3+} Cr^{6+} and W^{6+} (Wood et al., 2002; Palmer et al., 1987; Wesolowski et al., 1984). Similar facilities being developed by Scott Wood at the University of Idaho and Pascale Benezeth at CNRS, Toulouse promise to expand the impact of this powerful approach.

Salt and Pressure Effects on Isotopic Exchange:

Since their development in the early 1950's, stable isotope techniques have been extensively utilized to study the sources, fluxes, and paths of aqueous fluids, and the extent of phase separation and mineral deposition from aqueous fluids in active geothermal systems, ore deposits, metamorphic and magmatic rocks. The prerequisite to the successful application of stable isotope techniques to geothermal systems and other fluid-dominating geologic systems is basic knowledge of isotope fractionations between different phases and species (water, minerals, steam, gases, and dissolved species). It has usually been assumed that temperature is the sole variable controlling equilibrium fractionation of the stable isotopes of light elements (hydrogen, carbon, nitrogen, sulfur, etc.). Despite the discovery of the effect of dissolved salt on isotopic partitioning, "isotope salt effects," in the early 1950s, long-lasting controversy on the isotope salt effects at elevated temperatures was not resolved until the studies of Juske Horita, Dave Cole and Dave Wesolowski over the past several years (Horita et al., 1993a, 1993b, 1995) (Fig. 5).

The same is true for the effect of pressure on isotope partitioning. Our recent studies unequivocally demonstrate that pressure indeed affects isotopic partitioning between fluids and solids far beyond analytical errors (Horita et al., 1999; Horita et al., 2002) (Fig. 6). Thus, the isotope fractionation factor is a function not only of temperature, but also of pressure and fluid composition.

Beyond accurate knowledge of the three variables (T, P, X_{fluid}) in macroscopic isotope fractionation, we are expanding our efforts to advance our understanding of fundamental causes of the isotopic effects in various fluids and minerals at atomic- and molecular - levels under geologic and planetary conditions, including those at high-pressures and high-temperatures. We are employing a synergistic approach of laboratory experiments, theory, molecular-based simulations (Molecular-dynamics, Monte Carlo), and neutron diffraction - scattering methods. A recent result stemming from this approach published in *J. Chem. Phys.* by Chialvo and Horita (2003) presented the liquid-vapor and solid-vapor isotope fractionations of noble gases (Ne, Ar, & Kr) by means of (classical) molecular dynamics and Gibbs Ensemble Monte Carlo simulations (Fig. 7).

Fig. 10 MD simulation of water containing dissolved RbCl in contact with the rutile (110) surface at pH 8 (Predota et al., 2004b). The near surface structure of the solid is ab initio optimized (Bandura and Kubicki, 2003). The surface oxygen bonds are permitted to move with fixed ab initio bond lengths. Oxygen (red), hydrogen (white in bulk water, yellow when bound to surface oxygens) and titanium ions (grey) are reduced in size for clarity. The dark blue Rb^+ ions and pale blue chloride ions are shown at close to 'real' ionic radius. The first layer of Rb^+ ions are specifically bound in the tetradentate site and in contact with two bridging and two terminal hydroxyl groups. Rubidium and chloride ions are present further out in the EDL, but they do not occupy specific sites relative to the surface crystal structure, and are essentially 'diffuse' layer ions.

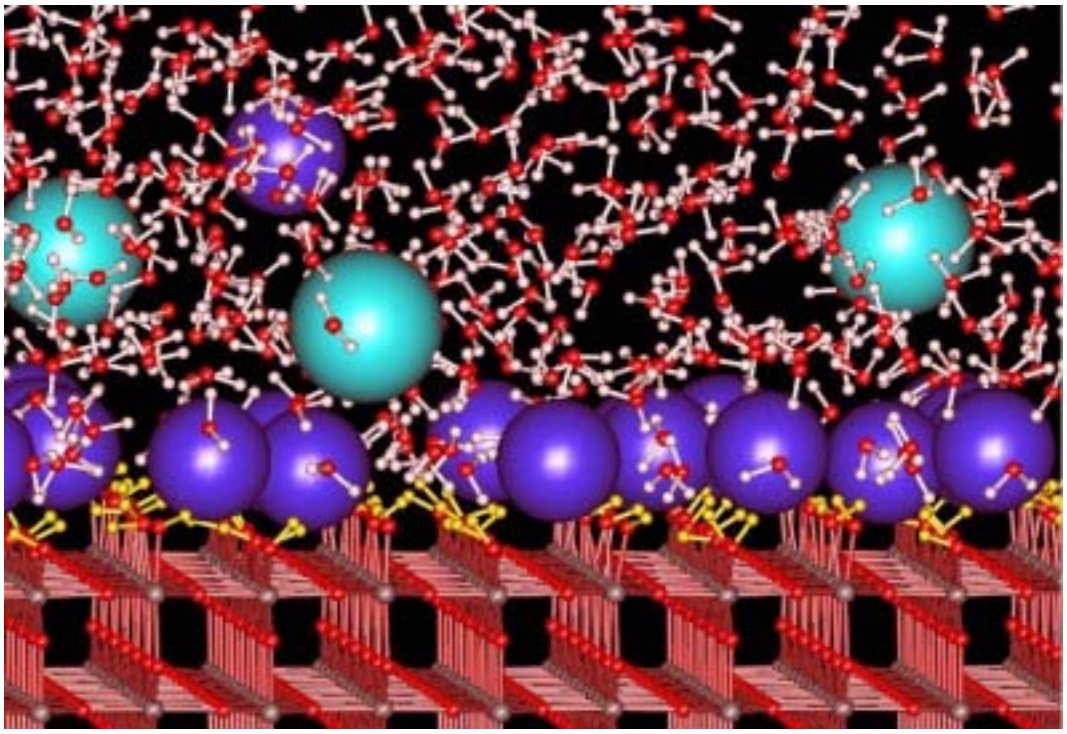

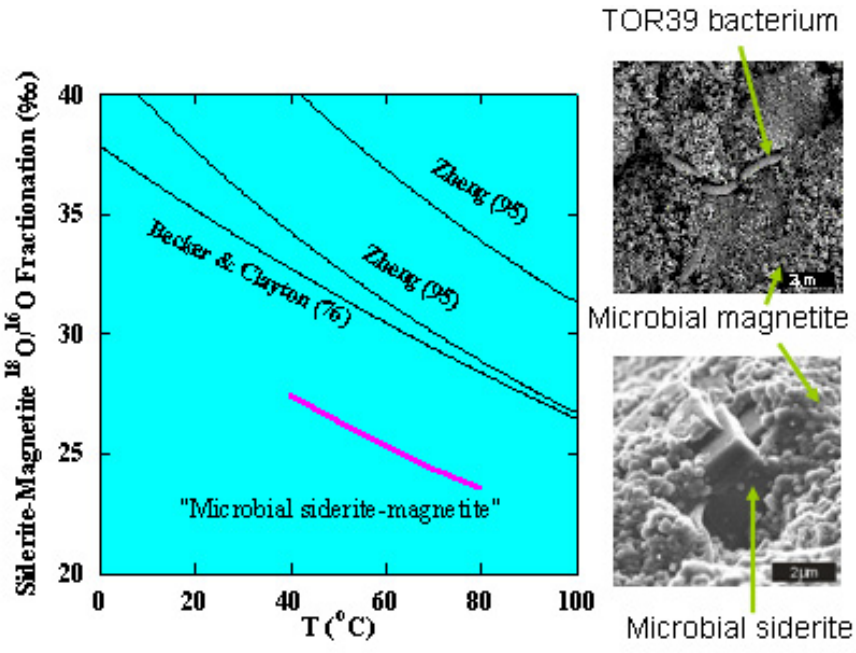

Fig. 11 $^{18}O/^{16}O$ fractionation between microbially precipitated magnetite and siderite (after Zhang et al., 2001).

INTERFACIAL PHENOMENA

Fluid/fluid and fluid/solid interfaces are regions across which all elemental transfers take place. Examples include water/gas, water/mineral, mineral/melt, coal/gas, gas/oil and water/oil interfaces. The complex structural and dynamic changes that occur at interfaces can profoundly affect hydrodynamics, reaction rates and reaction mechanisms. In this thrust area, we focus primarily on 'stable' interfaces, involving the juxtaposition of phases that largely retain their bulk characteristics at some distance from the interface. This enables us to isolate the unique features of the interface, which are controlled in part by changes in the compositions and state conditions of the bulk phases, whose structural and dynamic properties are often better understood.

Electrical charge develops on oxide and silicate surfaces in aqueous solutions due to the unsatisfied bond valence of the surface metal and oxygen atoms. Ions and water dipoles in solution are attracted to the charged surfaces, and the electrical double layer (EDL) thus formed influences the migration of dissolved species in subsurface brines as well as the stabilities and transport properties of colloids and the kinetics of dissolution and precipitation. Charge development and ion adsorption have been extensively studied by pH titrations and electrokinetic measurements of particle suspensions in aqueous electrolyte solutions. However, very few studies have been conducted at elevated temperatures, and almost none above 95˚C (Kosmulski 2001). Dave Wesolowski and Don Palmer, in collaboration with visiting scientists Mike Machesky and Moira Ridley have pioneered the first studies of the pH-dependent surface charge and pH_{pzc} (point of zero charge) of minerals at temperatures above 95˚C, including rutile (a-TiO_2) and magnetite (Fe_3O_4), by potentiometric titration (Machesky et al. 1998, Ridley et al. 2002, Wesolowski et al. 2000).

In the DOE Basic Energy Sciences project 'Nanoscale Complexity at the Oxide/Water Interface', Lead PI Dave Wesolowski is collaborating with a large group of ORNL and external researchers at Argonne National Lab, Illinois State Water Survey, Penn State, Vanderbilt, Texas Tech, St. Petersburg State University, University of South Bohemia (Czech Republic), Cardiff University, Wageningen in the Netherlands, and the University of Capetown to develop a molecular-level understanding of the EDL (Wesolowski et al., 2004). Figure 8 shows the point of zero charge of rutile as a function of temperature to 300˚C and the pH at which 50% of dissolved, multivalent trace ions in 1:1 electrolyte media are adsorbed on the mineral surface. This

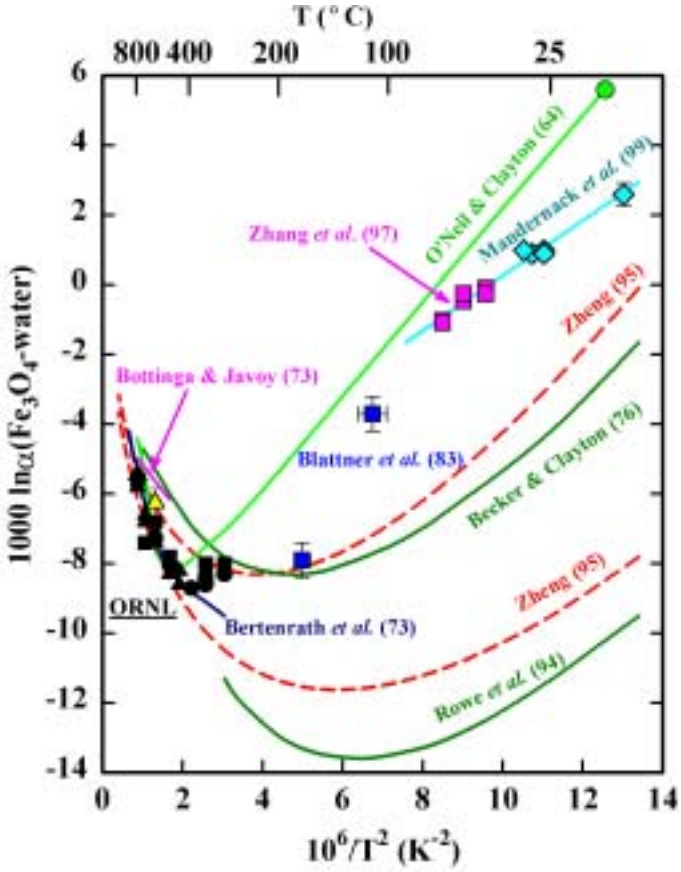

Fig. 12 Oxygen isotope fractionation between magnetite and water showing a comparison of high temperature data reported by Cole et al. (2004) with lower temperature results obtained in our studies using microbially- (squares) and inorganically-precipitated (solid circles) magnetite.

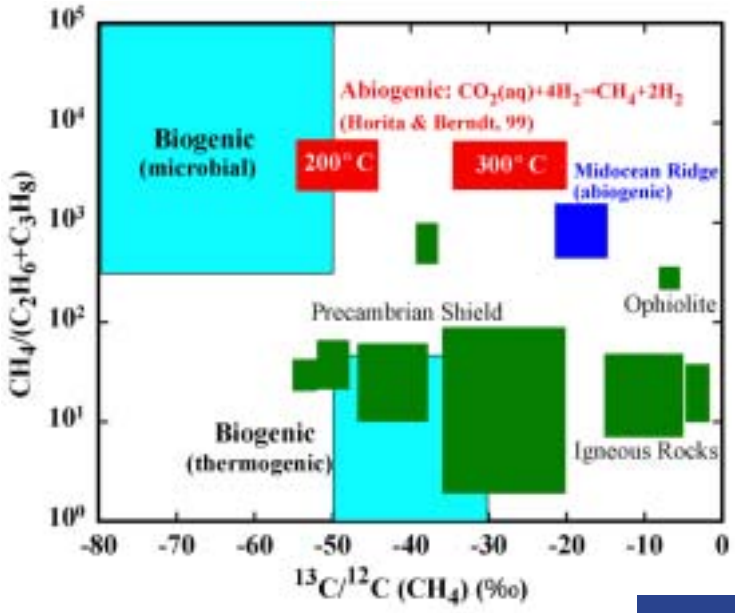

Fig. 13 CH_4 and light hydrocarbons produced abiotically under hydrothermal conditions. $^{13}C/^{12}C$ values and $C_1/(C_2+C_3)$ values of abiogenic hydrocarbons are indistinguishable from those of microbial gases (Horita and Berndt, 1999).

organic ion interactions with colloidal particles and single crystal surfaces; 3) second harmonic generation at single crystal/water interfaces; and 4) *ab initio* quantum calculations and molecular dynamics simulations of the mineral-solution interface. Figure 9 shows the sorption site geometries of cations at the rutile (110) surface in contact with liquid water containing the ions shown. We have found that all cations studied, including multivalent ions Ca^{2+}, Sr^{2+}, Zn^{2+}, and Y^{3+} and the cation of the background medium (Na^+, Rb^+) bind as 'inner sphere' species in direct contact with the surface bridging and terminal oxygen atoms, and that model-independent parameter gives a direct indication of the sorption affinities of these ions, which all increase with increasing temperature, at a rate considerably greater than the decrease in the point of zero charge with temperature, meaning that ion adsorption on mineral surfaces is even more important at elevated temperatures than at room temperature. Surface charge density for a given pH above or below the point of zero charge also increases with increasing temperature.

With support from this project, a high temperature zeta potential system has been developed by Serguei Lvov and co-workers at Penn State, and the pH_{iep} (isoelectric pH) of rutile and baddaleyite (ZrO_2) have been measured to 200˚C by microelectrophoresis (Fedkin et al. 2003). The team has also initiated a series of coordinated studies (cf. Zhang et al., 2004; Bandura and Kubicki, 2003; Ridley et al 2004; Predota et al., 2004a,b) in which pH-titration and electrokinetic data from powder suspensions are coupled with: 1) synchrotron X-ray standing wave (XSW) and crystal truncation rod (CTR) studies of single crystal surfaces in contact with electrolyte solutions; 2) neutron reflectivity and small angle scattering studies of

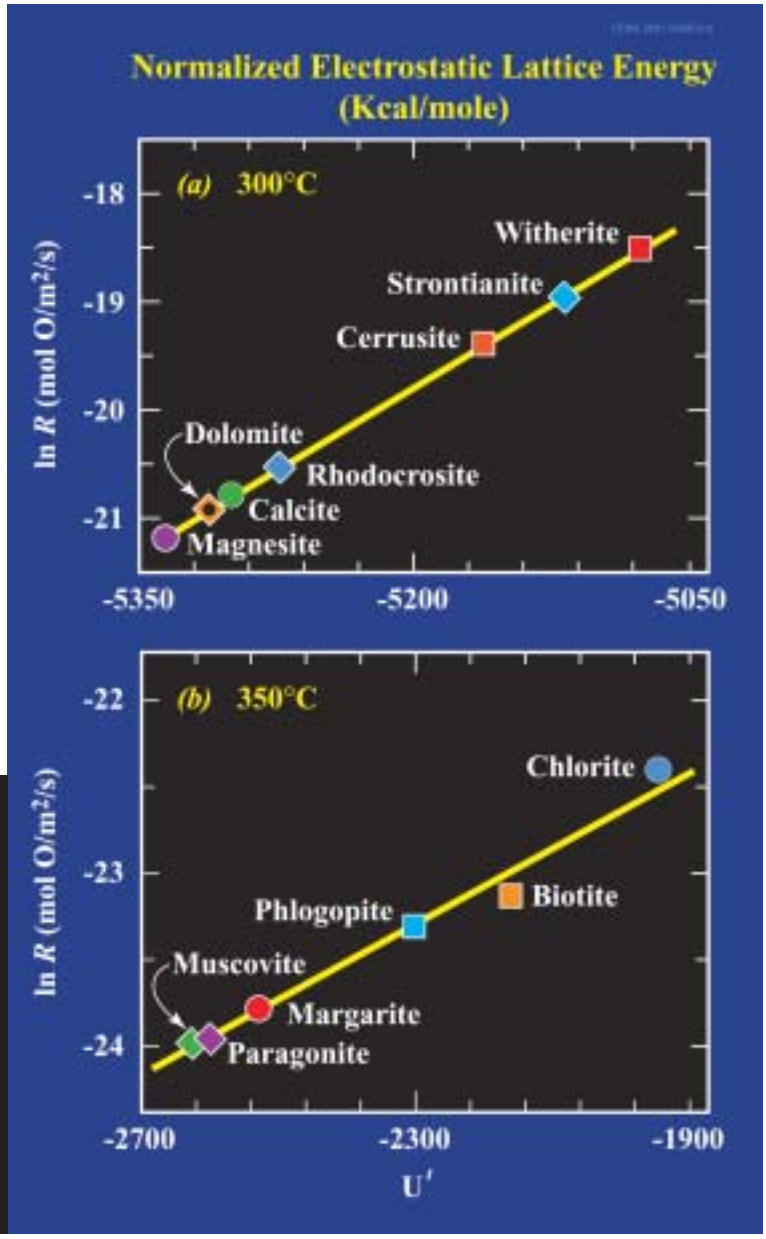

Fig. 14 Oxygen isotope exchange rates for metal carbonates (a) and layer silicates (b) reacted with pure H_2O at 300 and 350°C, respectively, plotted against the normalized electrostatic lattice energy (U'). U' represents the sum of electrostatic site potentials for each cation and anion normalized by dividing by the number of cations per unit formula in each phase. Experimental data are given for calcite, strontianite, witherite, chlorite, muscovite and biotite (Cole, 2000). Lattice energies have been calculated for phases common to each mineral group for which rate data are lacking. These have been projected to the lines regressed through the experimental data.

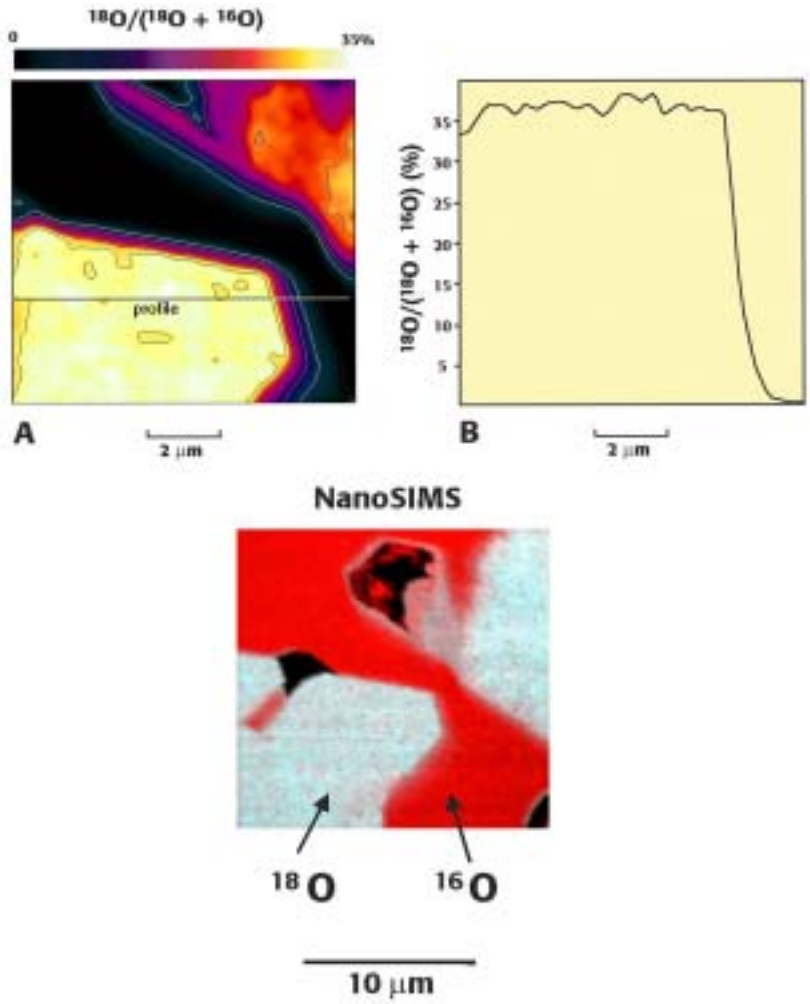

Fig. 15 (A) Contours of $^{18}O/(^{18}O+^{16}O)$ in replaced (via K-Na exchange) and unreacted albite, expressed as percent based on the detailed ion image given at the bottom. (B) Profile along the line shown in A. The ratio is uncorrected and is semiquantitative. The drop in the ratio occurs over a distance (several hundred nm) that is 5-10 times the spatial resolution of the NanoSIMS (Labotka et al., 2004b)

the radii of the ions largely dictate the specific geometry of their sorption sites, with the larger ions occupying 'tetradentate' sites involving two bridging and two terminal oxygens, and very small ions like Zn^{2+} forming mono- or bidentate complexes.

Figure 10 is based on an MD simulation of the interaction of Rb^{+} with the rutile (110) surface (Predota et al., 2004b). We have determined that the revised MUSIC model of surface protonation (Hiemsta et al., 1996), when optimized using *ab initio* bond lengths, is consistent with our experimental observations of the pH_{pzc} (Fitts et al., 2004), and that classical simulations of the rutile/water interface, optimized using *ab initio* surface charges and ion-surface oxygen interaction parameters are fully consistent with the X-ray results and compatible with Guoy-Chapman-Stern models of the EDL (Zhang et al., 2004; Bandura and Kubicki, 2003; Predota et al., 2004a,b). Significantly, for this surface, the influence of increasing ionic strength of weakly-bound ions such as Sr^{2+} (Figure 8) is shown to be a result of direct competition with background electrolyte cations (Na^{+}, Rb^{+}) for binding *at the same 'inner sphere' site*, rather than evidence of "outer sphere" binding of fully-hydrated species.

MINERAL-FLUID REACTIONS

The overarching goal of this thrust area is to understand, at both the microscopic and molecular-levels, the chemical and isotopic phenomena engendered by complex mineral-fluid interactions occurring over ranges of temperature and pressure relevant to the evolution of continental and oceanic crustal systems. Our approach is to obtain a quantitative understanding of the effects of specific environments and time scales on geochemical reactions in mineral-fluid systems through laboratory-based studies of simple, geologically-relevant systems, complemented by investigation of appropriate natural analogs. Predictive understand-

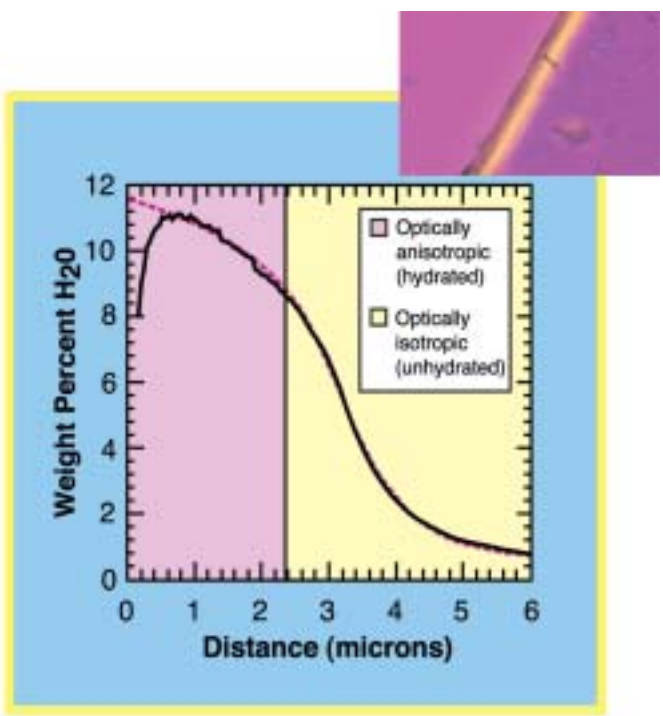

Fig. 16 Representative hydrogen diffusion profile in natural weathered Pachuca obsidian measured with ORNL's Camaeca 4f ion microprobe. The inset is a photomicrograph of the so-called "hydration rim" in a sample of weathered Pachuca obsidian. Note that this boundary is identified as a Becke line and is gradational, not sharp as assumed in the standard method of optical hydration dating (Anovitz et al. 1999).

(RIGHT) Fig. 17 Stepwise dissolution and precipitation rate studies of boehmite in equilibrium with a NaCl + NaOH + $NaAl(OH)_4$ solution at constant stoichiometric molal ionic strength of 0.1. The red curve is the equilibrium solubility of boehmite at this ionic strength and temperature reported by Palmer et al. (2001).

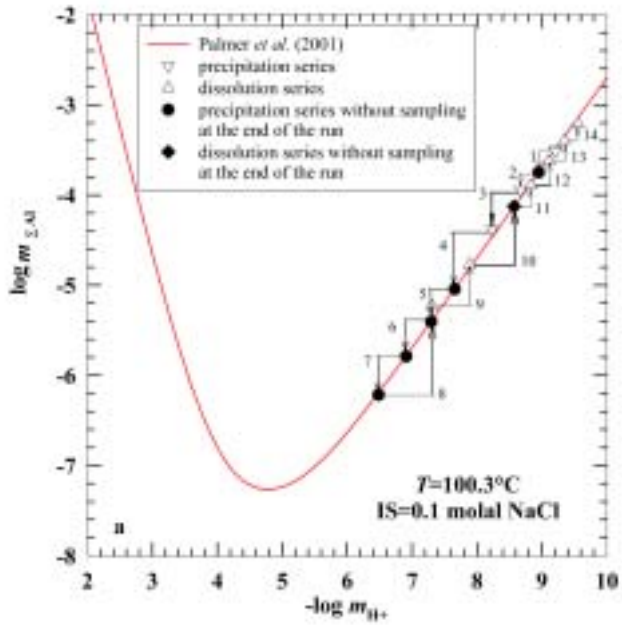

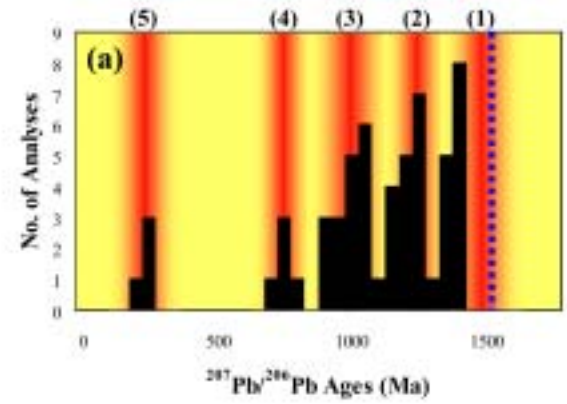

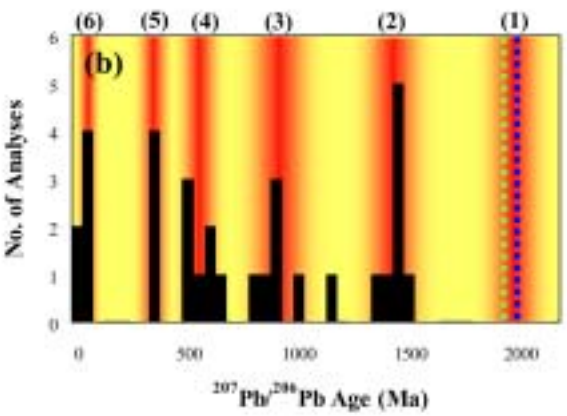

(LEFT) Fig. 18 Distribution of $^{207}Pb/^{206}Pb$ ages of uranium minerals determined by SIMS relative to major tectonic events that have affected (a) the Athabasca Basin region and (b) Francevillian Basin, host to the Oklo-Ok lobondo natural fission reactors. In (a), the black dash line represents the U-Pb age of the formation for the Athabasca uranium deposits (~1.6 Ga) and the numbers in parentheses mark the following tectonic events: (1) Accretion of Nena (~1.5.Ga); (2) Thermal emplacement of the McKenzie dike swarm (~1.3 Ga); (3) Accretion of Rodinia (~1.0 Ga); (4) Breakup of Rodinia (0.9-0.7 Ga); (5) Breakup of Pangea (~250 Ma). In (b), the dash line represents the U-Pb age of formation of the Oklo-Ok lobondo natural fission reactors (~2.0 Ga), the dotted line represents the U-Pb age for sustained fission reactions (i.e., criticality; ~1.95 Ga), and the numbers in parentheses mark the following tectonic events: (1) Accretion of Atlantica (~2.0 Ga); (2) basin uplift and carbonate diagenesis (~1.5 Ga); (3) Accretion of Rodinia (~1.0 Ga); (4) Accretion of Gondwana (~0.5 Ga); (5) Accretion of Pangea (~250 Ma); and (6) Breakup of Gondwana (~150-40 ma). These deposits represent one of the few areas in the world that have preserved a nearly complete neotectonic record of the continents over the past 1.5 Ga.

ing of these phenomena can contribute to the resolution of the long-standing problem of the inadequacy of simple assumptions of local equilibrium to represent accurately the observed geochemical record in natural systems. This thrust area is comprised of four sub-themes: isotopic fractionation in carbonate-, oxide- and silicate-fluid systems, mechanisms and rates of chemical and isotopic exchange, natural water-rock interaction analogs, and the influence of nano-confinement on fluid behavior.

Isotopic Fractionation:

In addition to the isotope salt and pressure effect studies described above, Cole and Horita have been involved in several studies designed to obtain accurate information on the partitioning of stable isotopes, both equilibrium and kinetic, for a number of key microbial and inorganic reactions, through systematic detailed laboratory experiments. For example, siderite ($FeCO_3$) was precipitated *in vitro* between 10 and 70˚C, mediated by thermophilic dissimilatory iron-reducing and fermentative bacteria sampled during deep subsurface drilling (Liu et al. 1997). Well-crystallized, nm-sized (10-100 nm), magnetite-rich (64-88 wt%) iron oxides were precipitated extracellularly after a few days of incubation. In the presence of $CO_2(aq)$, thermophilic fermentative and iron-reducing bacteria facilitated the precipitation of well-formed rhombs of siderite (several m across). Siderite-magnetite $^{18}O/^{16}O$ fractionation factors obtained by combining results from separate studies of microbial magnetite (Zhang et al., 1997) and siderite (Zhang at al., 2001) differ substantially from those in the literature (Zheng, 1999) (Fig. 11). In a complementary study, Cole et al. (2004) determined the oxygen isotope fractionation factors between magnetite and water at temperatures between 300 and 800°C. These new results have been plotted in Fig. 12 along with the lower temperature fractionation data obtained from both microbial and inorganic magnetite precipitation pathways.

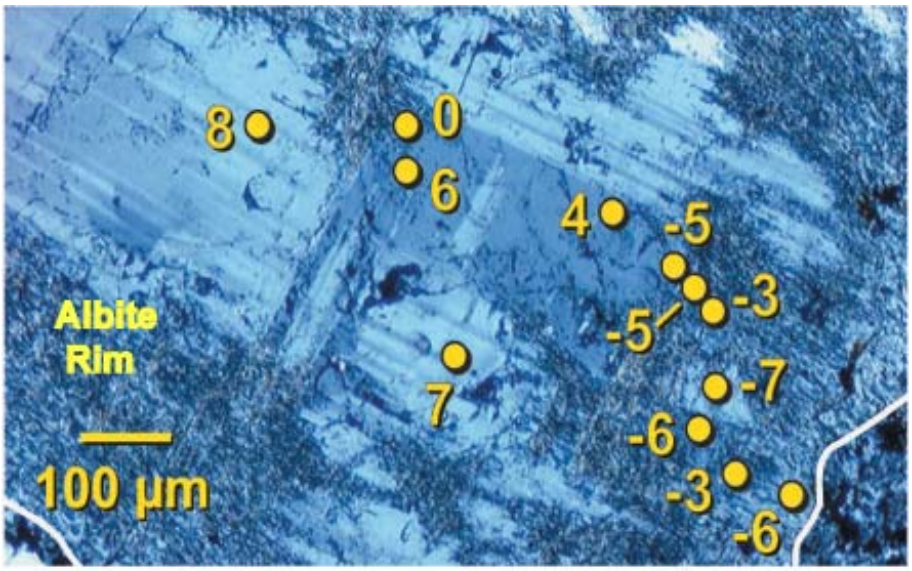

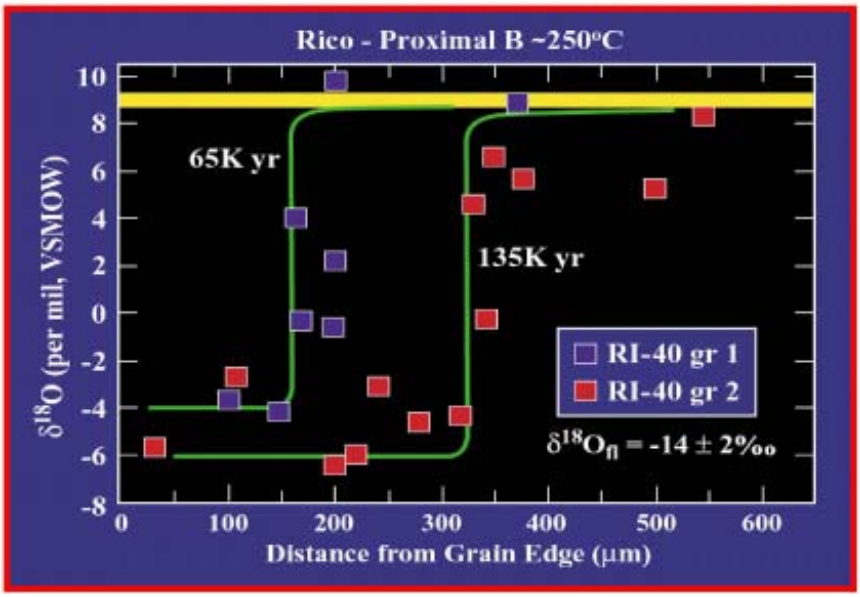

Fig. 19 (Upper) Representative photomicrograph of an altered plagioclase phenocryst from the intermediate temperature zone (200-250°C) in the Rico, CO paleo-hydrothermal system (Cole et al., 2004). Albite and minor muscovite compose mottled zones that typically rim unaltered plagioclase interiors. SIMS oxygen isotope data (rounded to the nearest per mil) are shown for spot sizes of ~25-30 mm in diameter. The value of 0ä near the interior is indicative of a case where isotopic exchange with isotopically light water (-14±2ä) can penetrate into the interior of grains along fractures. White lines in the lower left and right corners demarcate the grain edge. (Lower) Oxygen isotope compositions plotted versus distance from the grain edge for two different grains from the intermediate zone. Note the step function exhibited by both data sets indicative of an equilibrated rim and modestly sharp reaction front. The duration (in kyr) necessary to produce these fronts have been estimated with a coupled reaction-diffusion model that considers the position of the original grain edge fixed (pseudomorphic replacement).

Although the occurrence of deep-earth, mantle methane is still very controversial, there are an increasing number of reports suggesting the inorganic (abiogenic) formation of methane in the Earth's crust. We have experimentally investigated the mechanisms and isotopic fractionation during the abiogenic CH_4 formation from dissolved CO_2 under hydrothermal conditions (Horita and Berndt, 1999). Experiments were performed under conditions similar to those commonly encountered during the serpentinization of ultramafic rocks of the oceanic crust (200-400º C, 50 MPa). Our experimental results reveal that $\delta^{13}C$ values of abiogenic CH_4 formed from dissolved CO_2 can be very low, and may overlap values typical for microbial CH_4 (Fig. 13). In nature, Ni-Fe alloys, which are important phases in the paragenetic sequence of minerals that form during hydrothermal alteration of olivine-rich rocks, are rather widespread in nature (continental ultramafic settings, oceanic crustal environments, and meteorites). Thus, abiogenic methane formation via an awaruite/Ni-Fe alloy-catalyzed reaction may occur more commonly in the Earth's crust than is currently recognized.

Data on the oxygen and hydrogen isotope compositions of hydrous minerals provide a useful monitor of fluid-rock interaction in the Earth's crust. Rigorous interpretation of data generated from natural samples, however, requires accurate information of $^{18}O/^{16}O$ and D/H fractionation factors between minerals and water. Many of these have been summarized recently by Chacko et al. (2001) and Horita and Cole (2004). Using a variety of hydrothermal techniques we have reported on the fractionation factors between chlorite-water ($^{18}O/^{16}O$; Cole and Ripley, 1999), epidote-water (D/H; Chacko et al., 1999) and brucite-water (D/H; Horita et al., 2002).

Mechanisms and Rates of Isotopic Exchange:

A number of experimental, empirical and quasi-theoretical methods have been used to quantify the mechanisms and rates of isotopic exchange accompanying mineral transformations (growth, dissolution, chemical exchange), diffusion of light elements (O, C, H) in minerals, and transport of volatiles in glasses and melts (e.g. H_2O, SO_2). A detailed summary of the mechanisms and rates of isotopic exchange for many mineral and melt systems was given in Cole and Chakraborty (2001). We have investigated the dependency of rates of stable isotope exchange on temperature, pressure, fluid/volatile composition, fluid/solid ratios, and grain size for a number of mineral systems including calcite-H_2O-NaCl (Cole, 1992); calcite-CO_2 (Labotka et al., 2000,

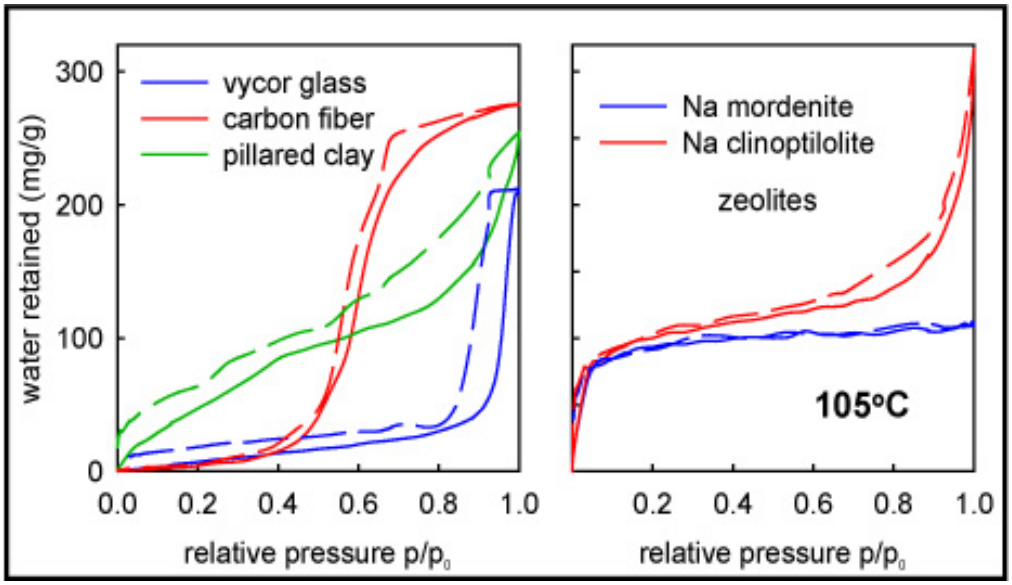

Fig. 20 Water adsorption (solid curves)-desorption (dashed curves) versus p/p_{sat} for a number of nano-porous solids (clay, silica, graphite, zeolites) at 105°C (Cole et al., 2004, Striolo et al., in press). ORNL's isopiestic apparatus was used to measure the water uptake and release as a function of temperature (up to 200°C) and pressure (vacuum to p_{sat} at a given T).

2004a); and metal carbonates [(Ca, Ba, Sr)-H_2O] and layer silicates (chlorite, muscovite, biotite-H_2O) (Cole, 2000). The influence of aqueous NaCl on oxygen isotope rates for calcite can be profound with an increase of nearly one order of magnitude (in units of moles O m^{-2} s^{-1}) with an increase in salinity of 1 molal. Pressure effect studies on calcite at a temperature of 500°C suggest that rate constants increase by about 0.4 log units per 100 MPa for the pure H_2O system, but only about 0.15 log units per 100 MPa at molalities between 1 and 4 (Cole, 1992). More recently, it has been noted by Cole (2000) that an increase in oxygen isotope exchange rates can be closely correlated with a decrease in the electrostatic lattice energies of select groups of minerals, i.e., carbonates and layer silicates (Fig. 14). By establishing an unambiguous relationship between rate, lattice energy, and ultimately, temperature, it should be possible to develop empirical equations useful in predicting rates of isotopic exchange for minerals for which experimental data are lacking.

We have used our Cameca 4f ion microprobe to measure the diffusivities of light elements in minerals and glasses via depth profiling. In collaboration with Ted Labotka at the University of Tennessee, Knoxville (UTK), diffusion of C and O has been measured in calcite reacted with pure $^{13}C^{18}O_2$ as a function of temperature at 100 MPa (Labotka et al., 2000) and pressure (0.1 to 200 MPa) between 500 and 800°C (Labotka et al., 2004). The ion microprobe has also been used to image the distribution of isotopic enrichments and depletions associated with chemical reactions. Amelia albite was reacted with 2 molal ^{18}O enriched solution of KCl at 600°C and 200 MPa (Labotka et al., 2004b). In collaboration with Frank Stadermann at Washington University, we showed from NanoSIMS images that the interface shows the distribution of ^{18}O and ^{16}O in the hydrothermally altered and unaltered albite. The data show that the exchange is not uniform and is controlled by the presence of fluid-filled cracks. Labotka et al. (2004b) also showed that the isotopic exchange rate is a function of the fluid-filled porosity.

(Below) Fig. 21 Representative results from Grand canonical Monte Carlo (GCMC) and MD simulation of H_2O adsorption-desorption in graphite slit-pores (Cole et al., 2004; Striolo et al., in press). This example shows simulated sorption curves of H_2O at 498K for a simulation box 4.6 x 4.4 x 4.2 nm with pores 0.6, 1.0 and 2.0 nm wide (center box). The MD-derived distributions of H_2O at two different stages of water uptake are given in the lower left and right. The trajectories of water movement in these pores are shown in the upper right. The density profiles for O and H are shown in the upper right inset for a 1 nm slit pore with a p/p_{sat} value >0.4. Note that above this value we predict capillary condensation and the formation of two distinct water layers stabilized by hydrogen bonds. The general geometry and hysteresis behavior predicted by our simulations match quite closely what we observe experimentally, as seen in Fig. 20.

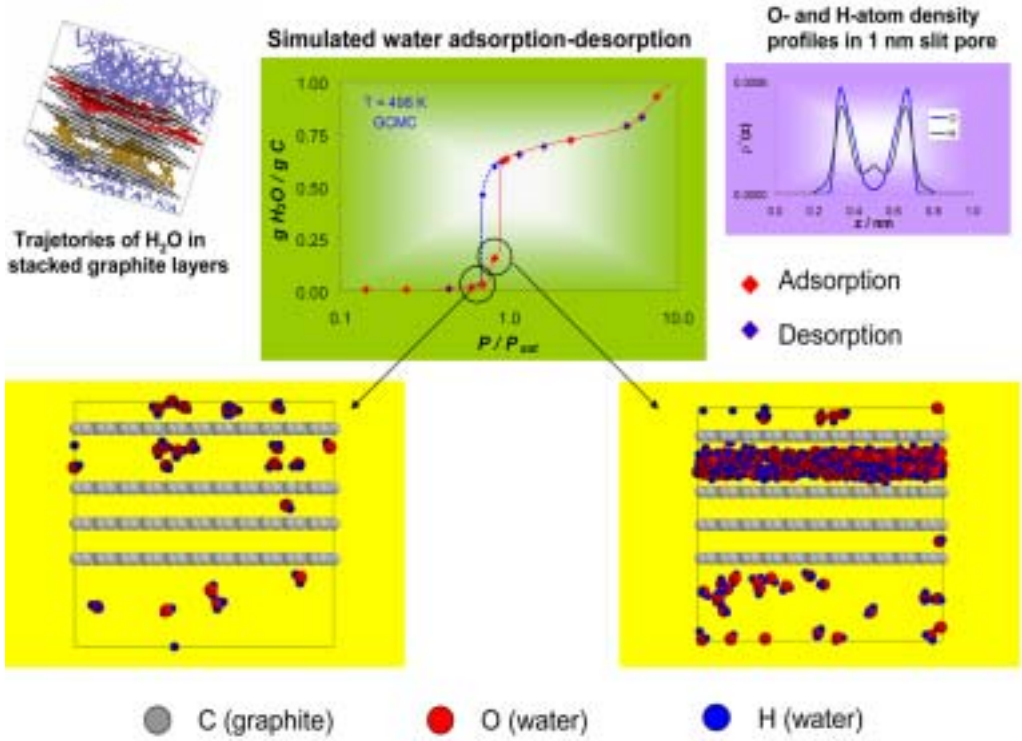

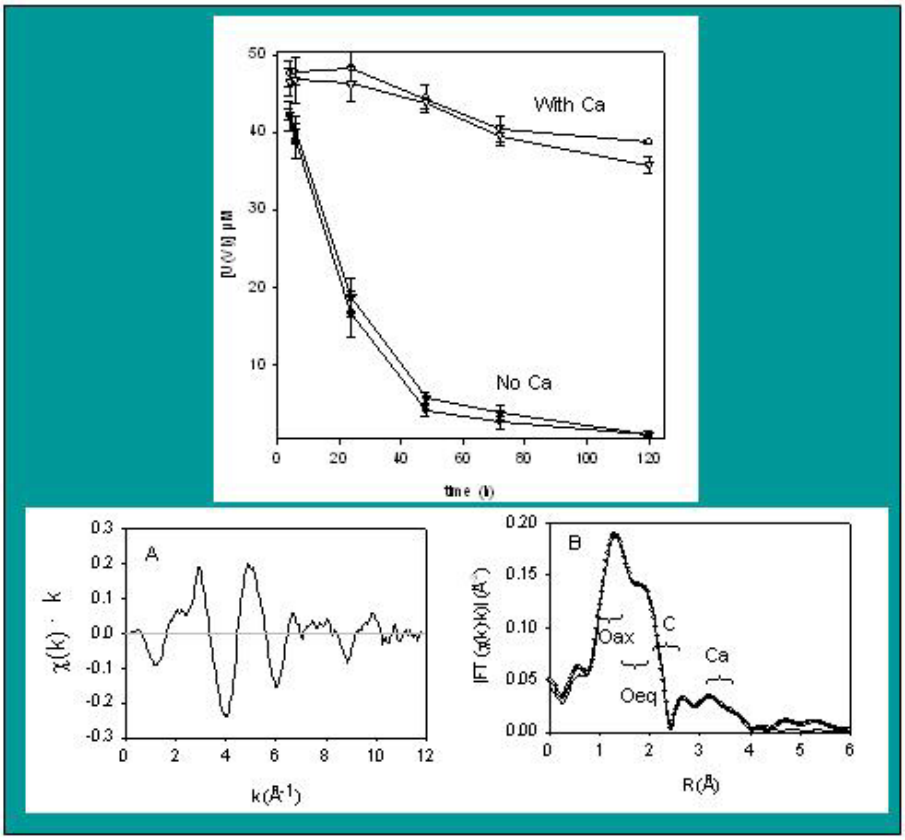

Fig. 22 Upper panel: Effect of Ca on U(VI) reduction by the obligate anaerobe* Desulfovibrio desulfuricans*; Lower panel: (a) XAFS χ(k) • k data for Ca-containing base solution. (b) Magnitude of the Fourier transform of the data shown in Fig. 1a (open circles) and best-fit model (thick line). Data processed with Δk = 3.3-9.3 -1, ΔR = 0.9-4.0 , and a Hanning window with a full sill width of 1.0 -1. Oax = axial oxygen; Oeq = equatorial oxygen (Brooks et al., 2003).

tion progress in dolomite reacted at high temperatures and pressures (up to 700°C and 200 MPa) (DeAngelis et al., 2003).

In one other interesting application of the ion microprobe, Riciputi and Cole, along with Larry Anovitz, Mike Elam and Mostafa Fayek of UTK debunked the long-standing industry of dating ancient glassy artifacts by using optically measured hydration rims formed from weathering (Anovitz et al. 1999; Riciputi et al., 2002; Anovitz et al. 2004b). Our ion microprobe work demonstrated that the true position of the hydration front was not coincident with the optical front at all, as had been originally assumed (Fig. 16). Armed with new experimental diffusion data on water in glass, which determines the rate of water migration into the glass, and measurements of water's true distribution in the glass, a new, more reliable dating method was proposed that capitalizes on the sensitivity of the ion probe.

Dissolution and Precipitation Rates:

Combining ORNL's unique high temperature pH measurement cells (Fig. 4) with specially-designed flow-through and batch solubility facilities, Dave Wesolowski, Don Palmer and Pascale Benezeth have conducted definitive studies of the equilibrium solubilities of gibbsite – $Al(OH)_3$, boehmite – AlOOH, and zincite – ZnO at temperatures of 0-300˚C and pressures from vapor saturation to a few hundred bars (Palmer et al., 2001; Benezeth et al, 2001, 2002; Wesolowski et al., 1998). Recently, we have been focusing on the near-equilibrium dissolution and precipitation rates of aluminum oxyhydroxides, silicates and carbonates, and the redox-metastable transformation of magnetite – Fe_3O_4 – to hematite – Fe_2O_3 in acidic solutions under highly reducing conditions, the latter in collaboration with Dr. Hiroshi Ohmoto and his students at Penn State. Figure 17 is an example of pH-step experiments that enable determination of the rate of dissolution and precipitation of boehmite at near-equilibrium conditions over a wide range of pH, in a single batch experiment. For simple reactions, such as the dissolution of boehmite in basic solutions, $AlOOH_c + 2H_2O = Al(OH)_4^- + H^+$, simple monitoring of the pH and application of charge and mass balance equations are found to be sufficient to calculate the instantaneous rate of dissolution and precipitation over wide ranges of pH, temperature, ionic strength and degree of super- or undersaturation, without the need to take samples.

Natural Analogs:

The ORNL CAMECA ims 4f ion microprobe lab specializes in high precision isotopic analysis of light elements (H, B, Li, C, O, and S) as well as heavy element isotopes (e.g., U-Th-Pb). Major developments with the ion microprobe include heavy and light element isotope measurements in radioactive minerals. In addition, geochemists at ORNL along with their university affiliated colleagues have developed and utilized the unique capabilities of the Neptune laser assisted multi-collector ICP-MS (LA-MC-ICP-MS), Triton thermal ionization mass spectrometry (TIMS), and JEOL HRTEM imaging to study a number of fundamental processes associated with fluid-rock interaction at the nanoscale, including both cation and anion diffusion, hydrogen storage capabilities of various materials, and nano-scale uranium mineral precipitation on bacterial surfaces. These developments are the basis of long term ongoing projects concerning crustal scale fluid-rock interactions.

For example, high precision (±0.2‰) Cu isotopic analyses of turquoise associated with igneous activity from the southwestern United States, by LA-MC-ICP-MS, show regional trends and up to 10‰ variation. On-going research is attempting to elucidate the fundamental processes causing these trends and the wide range in Cu isotopic values (Evans et al., 2004). Exploiting the unique *in situ* capabilities of the secondary ion mass spectrometry (SIMS) by developing isotope measurement techniques has led to results at the forefront of scientific investigations of crustal

scale fluid-rock interaction (Fayek et al 2002a, 2002b, 2003). Recent high spatial resolution (10-30 mm) *in situ* U, Pb, and O isotopic analyses, by SIMS, on U bearing minerals in sedimentary environments has revealed a wealth of detailed information corresponding to different paleo-fluid events associated with the large and economically significant sandstone basins including the age of orogenic events that resulted in large scale fluid events and mass transport. For example, *in situ* U-Pb and $^{207}Pb/^{206}Pb$ ages from U deposits indicate that uranium deposits can preserve a detailed record of large-scale fluid and thermal events, and may be sensitive to even larger tectonic events such as supercontinental cycles (Fig. 18). As most U deposits occur in sedimentary settings, these deposits offer one of the few approaches to developing a precise chronology of basin-scale fluid-rock events.

Similar ion probe studies have been conducted on the behaviour of oxygen isotopes in feldspars from different crustal settings. We have used oxygen isotope patterns in altered feldspars from the Rico, CO hydrothermal system (Fig. 19) to estimate the duration of fluid-rock interaction (Cole et al., 2004). The extent of albite rim formation and accompanying isotopic exchange vary across the system as a function of temperature, fluid isotope composition, and the local fluid-to-rock ratio. Formation times of reaction rims and associated isotopic patterns have been estimated with a coupled reaction-diffusion model that suggests that hotter (~250–350º C) hydrothermal circulation was active for ~100–300 k.y. in the center part of the system, perhaps only while the igneous "heat-engine" was still magma. Cooler (~150–200º C) circulation was widespread, lasting for >1,000 k.y. In collaboration with Claudia Mora at UTK, we have also determined the micro-spatial distribution of oxygen isotopes in feldspars from the Boehls Butte anorthosite, Idaho (Mora et al., 1999). The very large variations (up to ~15 per mil) with systematic gradients have been modelled as diffusive exchange between light meteoric water and original igneous feldspar at temperatures >500°C and pressures of 200-400 MPa.

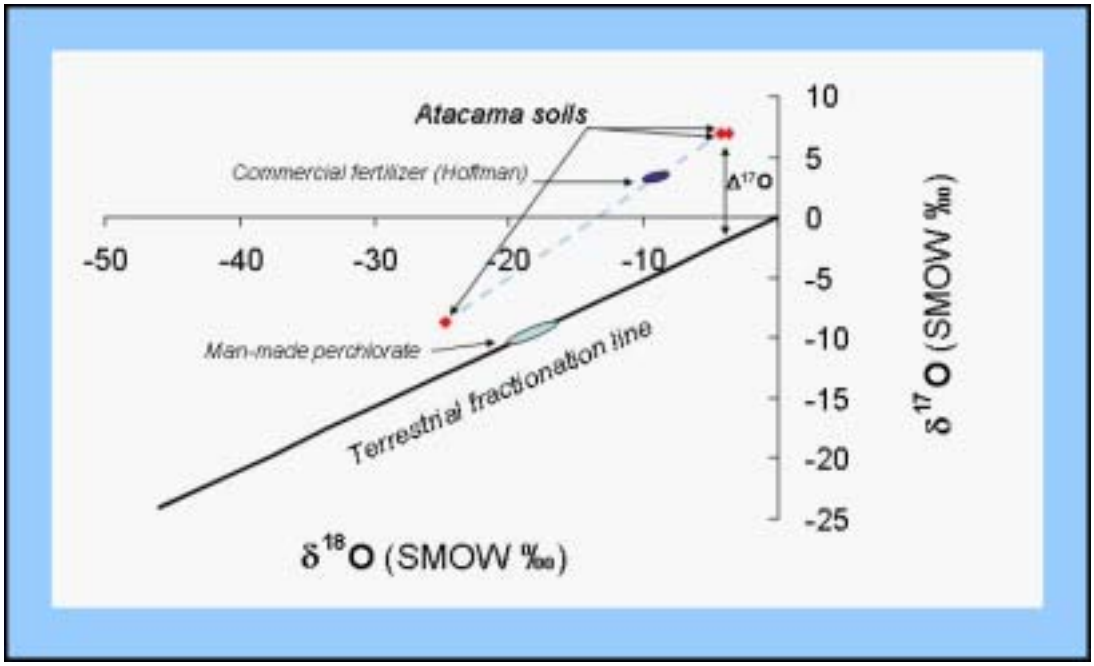

Fig. 23 $\delta^{18}O$–$\delta^{17}O$ plot for perchlorate from various man-made or natural sources including five reagent perchlorate salts, three different soils from the Central Depression of the central Atacama Desert, and a commercial nitrate fertilizer derived from Chilean salt deposits. Terrestrial fractionation line follows the mass-dependent fractionation relationship $\delta^{17}O = 0.52 \cdot \delta^{18}O$. The ^{17}O is the measure of the vertical deviation from this line (Bao and Gu, 2004).

Nanoporosity and Fluid Behavior:

Hydrocarbons, aqueous solutions, and gaseous species (e.g. CO_2, CH_4) can occupy the pores or fractures of numerous types of complex heterogeneous solids. The size, distribution and connectivity of these confined geometries, the chemistry of the solid, the chemistry of the fluids and their physical properties collectively dictate how fluids migrate into and through these micro- and nano-environments, wet and ultimately react with the solid surfaces. In order to assess key features of the fluid-matrix interaction at the nanoscale, a multidisciplinary approach was taken that employed neutron and X-ray scattering, simulations, and thermodynamic measurements to quantitatively describe the molecular properties of pure water, aqueous electrolytes and simple hydrocarbons confined to well-characterized porous media that serve as analogues to natural materials (Cole et al., 2004). Results have been obtained in four separate, but interrelated areas. Various types of microscopy (SEM; TEM) and scattering (SAXS, SANS) have been used to characterize a number of porous silicas, carbon fiber monoliths, zeolites and clays prior to interaction with fluids. Water adsorption/desoprtion isotherms have been determined on these materials up to 200°C (Fig. 20). FTIR, NMR and quasielastic neutron scattering (QENS) spectra have been obtained on water and, in the case of QENS, on electrolyte solutions (LiCl, $CaCl_2$, $NdCl_3$) confined in silica pore glass. SANS has been used to quantify the structural aspects related to critical phenomena of CO_2 confined to porous silica (Melnichenko et al., 2004; in press). Our simulation efforts (Grand canonical Monte Carlo; classical MD) thus far have focused on the adsorption and transport behavior of water and other volatiles such as CO_2 and CH_4 in slit pores geometries as a function of temperature (Fig. 21) composed of either carbon or mica (e.g., Striolo et al. in press). These studies conducted in concert are providing an understanding at the molecular level of how intrinsically different fluids behave in confined geometries compared to bulk

systems. If properly calibrated and scaled, an atomistic or molecular understanding of fluid-solid interaction may provide quantitative insight into the behavior of systems at the macroscopic scale.

ENVIRONMENTAL GEOCHEMISTRY

Contaminant Transport:

The Environmental Sciences Division at ORNL has a rich history of research in the area of contaminant transport – basic research to provide an improved understanding and predictive capability of the mechanisms governing the fate and transport of radionuclides and heavy metals in subsurface environments. Traditional methods such as batch and miscible displacement experiments are now complemented with a new generation of analytical capabilities to provide new insights into aqueous and water-mineral reactions. For example, the codisposal of radionuclides with anthropogenic chelating agents (e.g., EDTA) has been recognized as a factor contributing to the undesirable movement of radionuclides away from disposal areas. The stability of cobalt-EDTA (Co-EDTA) complexes, and thus the fate and transport of ^{60}Co in the subsurface, is strongly dependent on the oxidation state of Co (log $K_{Co(II)EDTA}$ = 18.3; log $K_{Co(III)EDTA}$ = 43.9). Oxidation of Co(II)EDTA to Co(III)EDTA by manganese oxides present in aquifer solids has been described but the identity of the reduced Mn product remained unresolved (Jardine et al., 1993; Jardine and Taylor, 1995). Using a novel hydrodynamic flow cell coupled with X-ray absorption near edge spectroscopy (XANES) we determined both the solution and solid phase species of cobalt and manganese in real time (Fendorf et al., 1999). Co(III)EDTA is produced while Mn(IV) in pyrolusite (β-MnO_2) is reduced to Mn(III) which forms an α-Mn_2O_3 layer on the pyrolusite. Consequently, this layer passivates the surface limiting the production of Co(III)EDTA after an initial reaction period. The XANES spectra clarified that Mn(III) is formed rather than Mn(II) resulting in the formation of a stable Mn(III) solid.

Biogeochemistry:

In recent years, a significant body of work has shown that dissimilatory metal-reducing bacteria (DMRB) can also reduce a number of toxic metals and radionuclides of environmental concern such as Cr(VI), U(VI), and Tc(VII). From the perspective of remediating contaminated environments, the bacterial reduction of these contaminants is desirable as the lower oxidation state species are less mobile and have a lower solubility than when present at higher oxidation states. Despite the promise of bioreduction as a remediation strategy, the factors that enhance or inhibit the rate and extent of biogeochemical U(VI) reduction under representative environmental conditions are not well defined. Only recently has the quantification of a few key interactions been established. For example, we recently reported the inhibition of bacterial U(VI) reduction by DMRB in the presence of environmentally realistic concentrations of soluble calcium (Ca) (Fig. 22) (Brooks et al., 2003). X-ray absorption fine structure (XAFS) measurements confirmed the presence of an aqueous Ca-U(VI)-CO_3 complex. Calcium, at millimolar concentrations, caused a significant decrease in the rate and extent of U(VI) reduction by both facultative and obligate anaerobic bacteria, putatively through the formation of the Ca-U(VI)-CO_3 complex. The results are consistent with the hypothesis that U is a less energetically favorable electron acceptor when the Ca-U(VI)-CO_3 complexes are present. By understanding these key reactions, more predictable and effective approaches can be established for in situ bioremediation of U under realistic field conditions.

Environmental Forensics:

Perchlorate, or ClO_4^-, disrupts the thyroid gland that regulates metabolism in adults and physical development in children and is increasingly being found in soil and water. It is used to make solid rocket propellant and explosives but also occurs naturally, as in nitrate soils from Chile used to make fertilizers, making the source sometimes difficult to trace. An award-winning system developed at Oak Ridge National Laboratory to clean up perchlorate pollution is now also helping scientists determine whether the contamination is natural or man-made (Bao and Gu, 2004). The process of removing perchlorate also purifies it, allowing the isolation and examination of trace quantities of the compound. Using stable isotope analysis, investigators compared naturally-occurring perchlorate from Chile's Atacama Desert to synthetic or manufactured samples. The natural type had a distinctly high and positive ^{17}O anomaly but a lower ^{37}Cl value (Fig. 23). The ORNL treatment system provides a tool for the identification and forensics of perchlorate contamination in the environment. In addition, the results provide evidence to support the hypothesis that oxidation of volatile chlorine by O_3 with the subsequent formation of $HClO_4$ can be a minor sink for atmospheric chlorine.

References

Anovitz, L.M., Blencoe, J.G., Joyce, D.B.and Horita, J. (1998) Precise measurements of the activity/composition relations of H_2O-CO_2 and H_2O-N_2 fluids at 500˚C, 500 bars. *Geochim. Cosmochim. Acta* **62**, 815-829.

Anovitz, L.M., Elam, J.M., Riciputi, L.R.and Cole, D.R. (1999) The failure of obsidian hydration dating: Sources, implications, and resolution. *J. Archaeol. Sci.* **26**, 735-752.

Anovitz, L.M., Labotka, T.C., Blencoe, J.G., and Horita, J. (2004a) Experimental determination of the activity-composition relations and phase equilibria of H_2O-CO_2-NaCl fluids at 500º C, 500 bars. *Geochim. Cosmochim. Acta* **68**, 3557-3567.

Anovitz, L.M., Elam, J.M., Riciputi, L.R. and Cole, D.R. (2004b) Isothermal time-series determination of the rate of diffusion of water in Pachuca obsidian. *Archaeometry* **46**, 301-326.

Bandura, A.V. and Kubicki, J.D. (2003) Derivation of force field parameters for TiO_2-H_2O systems from ab initio calculations. *J. Phys. Chem. B.* **107**, 11072-11081.

Bao, H. and Gu, B. (2004) Natural perchlorate has a unique oxygen isotope signature. *Environ. Sci. Technol.* **38,** 5073-5077.

Becker, R.H. and Clayton, R.N. (1976) Oxygen isotope study of a Precambiran banded iron-formation. Hamersley Range, Western Australia. *Geochim. Cosmochim. Acta* **40**, 1153-1165.

Benezeth, P., Palmer, D.A., Wesolowski, D.J. and Xiao, C. (2002) New measurements of the solubility of zinc oxide from 150 to 350˚C. *J. Solution Chem.* **31**, 947-973.

Benezeth, P., Palmer, D.A. and Wesolowski, D.J. (2001) Aqueous high-temperature solubility studies. II. The solubility of boehmite at 0.03 m ionic strength as a function of temperature and pH as determined by in situ measurements. *Geochim. Cosmochim. Acta* **65**, 2097-2111.

Benezeth, P., Palmer, D.A. and Wesolowski, D.J. (1997) Dissociation quotients of citric acid in aqueous sodium chloride media to 150˚C. *J. Solution Chem.* **26**, 63-84.

Bertenrath, R., Friedrichsen, H. and Hellner, E. (1973) Die fraktionierung der sauerstoffisotope $^{16}O/^{18}O$ im systemeisenoxidwasser. *Fortschr. Mineralogie* **50**, 32-33.

Blattner P., Braithwaite W.R. and Glover R.B. (1983) New evidence on magnetite oxygen isotope geothermometers at 175º C and 112º C in Wairakei steam pipelines (New Zealand). *Isotope Geosci.* **1**, 195-204.

Blencoe, J.G. (2004) The CO_2-H_2O system. IV. Empirical equations for representing vapor-liquid equilibria at 110-350º C. *Amer. Mineral.* **89**, 1447-1455.

Blencoe, J.G., Anovitz, L.M. and Singh, J. (2000) A semi-empirical excess pressure equation for CO_2-H_2O fluids at 400º C, 0-400 MPa. *Proceedings of the 13th International Conference on the Properties of Water and Steam*, 126-133.

Blencoe, J.G., Drummond, S.E., Seitz, J.C. and Nesbitt, B.E. (1996) A vibrating-tube densimeter for fluids at high pressures and temperatures. *Int. Jour. Thermophysics* **17**, 179-190.

Blencoe, J.G., Naney, M.T. and Anovitz, L.M. (2001) The CO_2-H_2O system. III. A new experimental method for determining liquid-vapor equilibria at high subcritical temperatures. *Amer. Mineral.* **86**, 1100-1111.

Blencoe, J.G., Seitz, J.C. and Anovitz, L.M. (1999) The CO_2-H_2O System. II. Calculated thermodynamic mixing properties for 400˚C, 0.1-400 MPa. *Geochim. Cosmochim. Acta* **63**, 2393-2408.

Bottinga Y. and Javoy M. (1973) Comments on oxygen isotope geothermometry. *Earth Planet. Sci. Lett.* **20**, 250-265.

Brooks, S.C., Fredrickson, J.K., Carroll, S.L., Kennedy, D.W., Zachara, J.M., Plymale, A.E., Kelly, S.D., Kemner, K.M. and Fendorf, S. (2003) Inhibition of bacterial U(VI) reduction by calcium. *Environ. Sci.Technol.* **37**, 1850-1858.

Chacko T, Cole D.R. and Horita, J. (2001) Equilibrium oxygen, hydrogen and carbon isotope fractionation factors applicable to geological systems. In Valley JW, Cole DR (eds.) Stable Isotope Chemistry, Rev in Mineralogy and Geochemistry **43**, 1-81.

Chacko, T., Riciputi, L.R., Cole, D.R. and Horita, J. (1999) A new technique for determining equilibrium hydrogen isotope fractionation factors using the ion microprobe: Application to the epidote-water system. *Geochim. Cosmochim. Acta* **63**, 1-10.

Chialvo A.A. and Horita J. (2003) Isotopic effect on phase equilibria of atomic fluids and their mixtures: A direct comparison between molecular simulation and experiment. *J. Chem. Phys.* **119**, 4458-4467.

Cole, D.R. (1992) Influence of solution composition and pressure on the rates of oxygen isotope exchange in the system: calcite - H_2O - NaCl at elevated temperatures. *Chem. Geol.* (Isotope Geoscience Section) **102**, 199-216.

Cole, D.R. (2000) Isotopic exchange in mineral-fluid systems. IV. The crystal chemical controls on oxygen isotope exchange rates in carbonate-H_2O and layer silicate-H_2O systems. *Geochim. Cosmochim. Acta* **64**, 921-931.

Cole, D.R. and Chakraborty, S. (2001), Rates and mechanisms of isotope exchange. In Valley JW, Cole DR (eds.) Stable Isotope Chemistry, *Rev in Mineralogy and Geochemistry* **43**, 83-223.

Cole, D.R. and Ripley, E.M. (1999) Oxygen isotope fractionation between chlorite and water from 170˚ to 350˚C: A preliminary assessment based on partial exchange and fluid/rock experiments. *Geochim. Cosmochim. Acta* **62**, 449-457.

Cole, D.R., Larson, P.B., Riciputi, L.R. and Mora, C.I. (2004) Oxygen isotope zoning profiles in hydrothermally altered feldspars: estimating the duration of water-rock interaction. *Geology* **32**, 29-32.

Cole, D.R., Horita, J., Polyakov, V.B., Valley, J.W., Spicuzza, M.J. and Coffey, D. (2004) An experimental and theoretical determination of oxygen isotope fractionation in the system magnetite-H_2O from 300 to 800ºC. *Geochim. Cosmochim. Acta* **68**, 3569-3585.

Cole, D.R., Gruszkiewicz, M.S, Simonson, J.M., Chialvo, A.A., Melnichenko, Y.B., et al. (2004) Influence of nanoscale porosity on fluid behavior. In (R.B. Wanty and R.R. Seal, eds.) *Proceedings of the 11th International Symposium on Water-Rock Interaction*, A.A. Balkema, Leiden, 735-739.

DeAngelis, M.T., Labotka, T.C., Anovitz, L.M., Cole, D.R. and Fayek, M. (2003) Experimental investigation of reaction and fluid transport in dolomite rock. *Amer. Geophys. Union.* Abstr., Fall Mtg., San Francisco.

Dickson, A.G., Wesolowski, D.J., Palmer, D.A. and Mesmer, R.E. (1990) Dissociation constants of bisulfate ion in aqueous sodium chloride solutions to 250˚C. *J. Phys. Chem.* **94**, 7978-7985.

Duan Z., Møller N. and Weare J.H. (1992a) An equation of state for the CH_4-CO_2-H_2O system: I. Pure systems from 0 to 1000º C and 0 to 8000 bars. *Geochim. Cosmochim. Acta* **56**, 2605–2618.

Duan Z., Møller N. and Weare J.H. (1992b) An equation of state for the CH_4-CO_2-H_2O system: II. Mixtures from 50 to 1000º C and 0 to 1000 bars. *Geochim. Cosmochim. Acta* **56**, 2619–2631.

Evans, M.J., Fayek, M., Riciputi, L.R., Anovitz, L.M., Hull, S., Mathien, F.J. and Milford, H. (2004) LA-MC-ICPMS Determination of Copper Isotope Ratios in Turquoise from the Southwestern United States. *Eos Trans. AGU, **85***, Abstract V51A-0514.

Fayek, M., Utsunomiya, S., Ewing, R.C., Jensen, K.A. and Riciputi, L.R. (2003) The link between nanostructures and oxygen isotopic composition of uraninite at Oklo natural fission reactors, Gabon. *Am. Min.*. **88**, 1583-1590.

Fayek, M., Kyser, T.K. and Riciputi, L.R. (2002a) U and Pb isotope analysis of uranium minerals by ion-microprobe and the geochronology of the McArthur River and Sue Zone uranium deposits, Saskatchewan Canada. *Can. Min.* **40**, 1717-1733.

Fayek, M., Jensen, K.A., Ewing, R.C. and Riciputi, L.R. (2002b) In situ isotopic analysis of uraninite microstructures from the Oklo-Ok lobondo natural fission reactors, Gabon. *Materials Research Society Proceedings* **713**, 849-856.

Fedkin, M.V., et al. (2003) High temperature microelectrophoresis studies of the rutile/aqueous solution interface. *Langmuir* **19**, 3797-3804.

Fendorf, S., Jardine, P.M., Patterson, R.R., Taylor, D.L. and Brooks, S.C. (1999) Pyrolusite surface transformations measured in real-time during reactive transport of Co(II)$EDTA^{2-}$. *Geochim. Cosmochim. Acta* **63**, 3049-3057.

Fitts, J.P., Machesky, M.L., Wesolowski, D.J., Shang, X., Kubicki, J.D., Flynn, G.W., Heinz, T.F. and Eisenthal, K.B. (in review) Second harmonic generation at the water-rutile (110) interface confirms MUSIC model prediction of surface protonation. *Chem. Phys. Let.* (submitted).

Friend, D.G., Harvey, A.H., Marshall, S.L. and Blencoe, J.G. (2004) Chapter 6. Vapor-liquid equilibrium Involving aqueous, binary nonelectrolytes. In: Palmer, D. A., Fernandez-Prini, R., and Harvey, A. H. (eds.), *Aqueous Systems at Elevated Temperatures and Pressures: Physical Chemistry in Water, Steam and Hydrothermal Solutions*, 183-203.

Hiemstra, T., Venema, P. and van Riemsdijk, W.H. (1996) Intrinsic proton affinity of reactive surface groups of metal (hydr)oxides: The bond valence principle. *J. Colloid and Interface Sci.* **184**, 680-692.

Holloway J.R. (1977) Fugacity and activity of molecular species in supercritical fluids. In *Thermodynamics in Geology* (ed., D. G. Fraser), pp. 161–181. D. Reidel.

Horita J. and Berndt M.E. (1999) Abiogenic methane formation and isotopic fractionation under hydrothermal conditions. *Science* **285**, 1055-1057.

Horita, H. and Cole, D. R. (2004) Chapter 9. Stable isotope partitioning in aqueous and hydrothermal systems at elevated temperatures. In: Palmer, D. A., Fernandez-Prini, R., and Harvey, A. H. (eds.), *Aqueous Systems at Elevated Temperatures and Pressures: Physical Chemistry in Water, Steam and Hydrothermal Solutions*, 277-319.

Horita J., Wesolowski D.J. and Cole D.R. (1993a) The activity-composition relationship of oxygen and hydrogen isotopes in aqueous salt solutions. I: Vapor-liquid water equilibration of single salt solutions from 50 to 100º C. *Geochim. Cosmochim. Acta* **57**, 2797-2817.

Horita J., Cole D.R. and Wesolowski D.J. (1993b) The activity-composition relationship of oxygen and hydrogen isotopes in aqueous salt solutions. II: Vapor-liquid water equilibration of mixed salt solutions from 50 to 100º C and geochemical implications. *Geochim. Cosmochim. Acta* **57**, 4703-4711.

Horita J., Cole D.R. and Wesolowski D.J. (1995) The activity-composition relationship of oxygen and hydrogen isotopes in aqueous salt solutions. III: Vapor-liquid water equilibration of NaCl solutions to 350º C. *Geochim. Cosmochim. Acta* **59**, 1139-1151.

Horita J., Driesner T. and Cole D.R. (1999) Pressure effect on hydrogen isotope fractionation between brucite and water at elevated temperatures. *Science* **286**, 1545-1547.

Horita J., Cole D.R., Polyakov V.B. and Driesner T. (2002) Experimental and theoretical study of pressure effects on hydrogen isotope fractionation in the system brucite-water at elevated temperatures. *Geochim. Cosmochim. Acta* **66**, 3769-3788

Jardine, P.M., Jacobs, G.K. and O'Dell, J.D. (1993) Unsaturated transport processes in undisturbed heterogeneous porous media: II. Co-contaminants. *Soil Sci. Soc. Am. J.* **57**, 954-962.

Jardine, P.M. and Taylor, D.L. (1995) Kinetics and mechanisms of Co(II)$EDTA^{2-}$ oxidation by pyrolusite. *Geochim. Cosmochim. Acta* **59**, 4193-4203.

Kerrick D.M. and Jacobs G.K. (1981) A modified Redlich-Kwong equation for H_2O, CO_2, and H_2O-CO_2 mixtures at elevated pressures and temperatures. *Am. J. Sci.* **28**1, 735–767.

Kosmulski, M., *Chemical Properties of Material Surfaces*, Marcel Dekker, New York, 768p. (2001).

Labotka, T., Cole, D.R. and Riciputi, L.R. (2000) Diffusion of C and O in calcite at 100 MPa. *Am. Min.* **85**, 488-494.

Labotka, T.C., Anovitz, L.M. and Blencoe, J.G. (2002) Pore pressure during metamorphism of carbonate rock: effect of volumetric properties of H_2O-CO_2 mixtures. *Contrib. Mineral. Petrol.* **144**, 305-313.

Labotka, T.C., Cole, D.R., Riciputi, L.R. and Fayek, M. (2004a) Diffusion of C and O in calcite from 0.1 to 200 MPa. *Am. Min.* **89**, 799-806.

Labotka, T.C., Cole, D.R., Fayek, M., Riciputi, L.R. and Stadermann, F. (2004b) Coupled cation and oxygen isotope exchange between alkali feldspar and aqueous chloride solution. *Am. Min.* **89**, 1822-1825.

Liu, S., Zhou, J., Zhang, C., Cole, D.R., Gajdarziska-Josifovska, M. and Phelps, T. J. (1997) Novel thermophilic Fe(III)-reducing bacteria and their evolutionary implications. *Science* **277**, 1106-1109.

Machesky, M.L., Wesolowski, D.J., Palmer, D.A. and Hayashi, K.-I. Potentiometric titrations of rutile suspensions to 250˚C. *J. Colloid and Interface Sci.* **200**, 298-309 (1998).

Mandernack, K.W., Bazylinski, D.A., Shanks, W.C., III and Bullen, T.D. (1999) Oxygen and iron isotope studies of magnetite produced by magnetotactic bacteria. *Science* **285**, 1892- 1896.

Melnichenko, Y.B., Wignall, G.D., Cole, D.R. and Frielinghaus, H. (2004) Density fluctuations near the liquid-gas critical point of a confined fluid. *Phys. Rev. E.* **69**, 057102.

Melnichenko, Y.B., Wignall, G.D., Cole, D.R., Frielinghaus, H. and Bulavin, L. A. (2005) Liquid-gas critical phenomena under confinement: small-angle neutron scattering studies of CO_2 in aerogel. (accepted to *J. Molec. Liquids.*).

Mesmer, R.E., Baes, C.F., Jr. and Sweeton, F.H. (1970) Acidity measurements at elevated temperatures. IV Apparent dissociation product of water in 1 m potassium chloride up to 292˚C. *J. Phys. Chem.* **74**, 1937-1942.

Mesmer, R.E., et al. (1997) Experimental Studies in High Temperature Aqueous Chemistry at Oak Ridge National Laboratory. *Pure and Applied Chemistry* **69**, 905-914.

Mora, C.I., Riciputi, L.R. and Cole, D.R. (1999) Short-lived oxygen diffusion during hot, deep-seated meteroric alteration of anorthosite. *Science* **286**, 2323-2325.

O'Neil, J.R and Clayton, R.N. (1964) Oxygen isotope geothermometry. In Isotopic and Cosmic Chemistry, (eds. H. Craig, S. L. Miller, and G. J. Wasserburg), North-Holland, Amsterdam.

Palmer, D.A., Fernandez-Prini, R. and Harvey, A.H. (2004) *Aqueous Systems at Elevated Temperatures and Pressures: Physical Chemistry in Water, Steam and Hydrothermal Solutions*, Elsevier Academic Press, Amsterdam 753p.

Palmer, D.A., Wesolowski, D.J. and Mesmer, R.E. (1987) A potentiometric investigation of the hydrolysis of chromate (VI) ion in NaCl media to 175˚C. *J. Solution Chem.* **16**, 443-463.

Palmer, D.A., B n zeth, P. and Wesolowski, D.J. (2001) Aqueous high-temperature solubility studies. I. The solubility of boehmite as functions of ionic strength (to 5 molal, NaCl), temperature (100-290˚C) and pH as determined by in situ measurements. *Geochim. Cosmochim. Acta* **65**, 2081-2095.

Predota, M., Bandura, A.V., Cummings, P.T., Kubicki, J.D., Wesolowski, D.J., Chialvo, A.A. and Machesky, M.L. (2004) Electrical double layer at the rutile (110) surface. 1. Structure of the surfaces and interfacial water from molecular dynamics by use of ab initio potentials. *J. Phys. Chem. B.* **108**, 12049-12060.

Predota, M., Zhang, Z., Fenter, P., Wesolowski, D.J. and Cummings, P.T. (2004) Electrical double layer at the rutile (110) surface. 2. Adsorption of ions from molecular dynamics and X-ray experiments. *J. Phys. Chem. B.* **108**, 12061-12072.

Riciputi, L.R., Ingeneri, K., Hedberg, P.M.B. and Turgeon, S. (2004) The High Efficiency Cavity Source for Isotopic Analysis of Small Samples. *32nd International Geologic Congress*, Aug. 20-28, Florence, Italy.

Ridley, M.K., Wesolowski, D.J., Palmer, D.A. and Kettler, R.M. (1999a) Association quotients of aluminum sulphate complexes in NaCl media from 50 to 125˚C: Results of a potentiometric and solubility study. *Geochim. Cosmochim. Acta* **62**, 459-472.

Ridley, M.K., Machesky, M.L., Wesolowski, D.J. and Palmer, D.A. (1999b) Calcium adsorption at the rutile-water interface: A potentiometric study in NaCl media to 250˚C. *Geochim. Cosmochim. Acta* **63**, 3087-3096.

Ridley, M.K, Machesky, M.L., Palmer, D.A. and Wesolowski, D.J. (2002) Potentiometric studies of the rutile-water interface: hydrogen-electrode concentration-cell versus glass-electrode titrations. *Colloids and Surfaces A* 204, 295-308.

Rowe, M.W., Clayton, R.N. and Mayeda, T.K. (1994) Oxygen isotopes in separated components of CI and CM meteorites. *Geochim. Cosmochim. Acta* **58**, 5341-5347.

Seitz, J.C. and Blencoe, J.G. (1999) The CO_2-H_2O System. I. Experimental determination of volumetric properties at 400˚C, 10-100 MPa. *Geochim. Cosmochim. Acta* **63**, 1559-1569.

Striolo, A., Gubbins, K.E., Gruszkiewicz, M.S., Cole, D.R., Simonson, J.M., Chialvo, A.A., Cummings, P.T., Burchell, T.D. and More, K.L. (in press) Temperature effect on water adsorption in porous carbons. (*Fluid Phase Equilibria*).

Wesolowski, D., Drummond, S.E., Mesmer, R.E. and Ohmoto, H. (1984) Hydrolysis equilibria of tungsten (VI) in aqueous sodium chloride solutions to 300˚C. *Inorg. Chem.* **23**, 1120-1132.

Wesolowski, D.J., Machesky, M.L., Palmer, D.A. and Anovitz, L.M. (2000) Magnetite surface charge studies to 290˚C from in situ pH titrations. *Chem. Geol.* **167**, 193-229 (2000).

Wesolowski, D.J., et al. (2004) Temperature effects and structure at the rutile-water interface. In (R.B. Wanty and R.R. Seal, eds.) *Proceedings of the 11th International Symposium on Water-Rock Interaction*, A.A. Balkema, Leiden, pp. 775-779.

Wesolowski, D.J., B n zeth, P. and Palmer, D.A. (1998) ZnO solubility and Zn^{2+} complexation by chloride and sulfate in acidic solutions to 290˚C with in situ pH measurement. *Geochim. Cosmochim. Acta* **62**, 971-984.

Wood, S.A, Palmer, D.A., Wesolowski, D.J. and B n zeth, P. (2002) The aqueous geochemistry of the rare earth elements and yttrium. Part XI. The solubility of $Nd(OH)_3$ and hydrolysis of Nd^{3+} from 30 to 290˚C at saturated vapor pressure with in situ pH_m measurement. In (R. Hellmann and S.A. Wood, eds.) *Water-Rock Interactions, Ore Deposits, and Environmental Geochemistry: A Tribute to David A. Crerar*, The Geochemical Society, Special Publication No. 7, pp. 229-256.

Xiao, C., Wesolowski, D.J. and Palmer, D.A. (2002) Formation quotients of aluminum sulfate complexes in $NaCF_3SO_3$ media at 10, 25 and 50˚C from potentiometric titrations using a mercury/mercurous sulfate electrode concentration cell. *Environ. Sci. Technol.* **36**, 166-173.

Zhang, C.L., Liu, S., Phelps, T.J., Cole, D.R., Horita, J., Fortier, S.M., Elless, M. and Valley, J.W. (1997) Physicochemical, mineralogical, and isotopic characterization of magnetic oxides formed by thermophilic iron-reducing bacteria. *Geochim. Cosmochim. Acta* **61**, 4621-4632.

Zhang C.L., Horita J., Cole D.R., Zhou J., Lovley D.R. and Phelps T.J. (2001) Temperature-dependent oxygen and carbon isotope fractionations of biogenic siderite. *Geochim. Cosmochim. Acta* **65**, 2257-2271.

Zhang, Z, et al. (2004) Ion adsorption at the rutile-water interface: Linking molecular and macroscopic properties". *Langmuir* **20**, 4954-4969.

Zheng, Y.F. (1995) Oxygen isotope fractionation in magnetites: structural effect and oxygen inheritance. *Chem.Geol.* (Isotope Geoscience Sect.) **121**, 309-316.

Zheng, Y.F. (1999) Oxygen isotope fractionation in carbonate and sulfate minerals. *Geochem. J.* **33**, 109-126.